POLITECNICO DI TORINO
Repository ISTITUZIONALE

Refined multilayered beam, plate and shell elements based on Jacobi polynomials

(Article begins on next page)

18 April 2024

Refined multilayered beam, plate and shell elements based on Jacobi polynomials

E. Carrera^{a,b*}, R. Augello^{a†}, A. Pagani^{a‡}, D. Scano^{a§}

$^a Mul^2$ Group

Department of Mechanical and Aerospace Engineering, Politecnico di Torino
Corso Duca degli Abruzzi 24, 10129 Torino, Italy.

^{b}Department of mechanical engineering, College of engineering,
Prince Mohammad Bin Fahd University P.O. Box 1664. Al Khobar 31952.
Kingdom of Saudi Arabia

Abstract: *In this paper, theories of structures based on hierarchical Jacobi expansions are explored for the static analysis of multilayered beams, plates and shells. They belong to the family of classical orthogonal polynomials. This expansion is employed in the framework of the Carrera Unified Formulation (CUF), which allows to generate finite element stiffness matrices in a straightforward way. CUF allows also to employ both layer-wise and equivalent single layer approaches in order to obtain the desired degree of precision and computational cost. In this work, CUF is exploited for the analysis of one-dimensional beams and two-dimensional plates and shells, and several case studies from the literature are analysed. Displacements, in-plane, transverse and shear stresses are shown. In particular, for some benchmarks, the shear stresses are calculated using the constitutive relations and the stress recovery technique. The obtained results clearly show the convenience of using equivalent single layer models when calculating displacements, in-plane stresses and shear stresses recovered by three-dimensional indefinite equilibrium equations. On the other hand, layer-wise models are able to accurately predict the structural behaviour, even though higher degrees of freedom are needed.*

Keywords: Composite structures; Layer-Wise, Equivalent Single Layer; Beam models, Plate models, Shell models; Jacobi polynomials; Stress Recovery.

1 Introduction

Layered structures have a leading role in several engineering applications, e.g. aerospace, biomedical and automotive. With the development of increasingly complex components, the need has arisen for a method which can simulate the behaviour of these structures. The anisotropy of the material represents a challenging issue in the development of this method,

---

*Full Professor. E-mail: erasmo.carrera@polito.it
†Assistant Professor. Corresponding author. E-mail: riccardo.augello@polito.it
‡Associate Professor. E-mail: alfonso.pagani@polito.it
§PhD. E-mail: daniele.scano@polito.it

since it causes intricate mechanical phenomena. Moreover, the shear stresses must respect the condition of continuity at each interface layer, whereas discontinuous mechanical properties in the transverse direction produce the zig-zag distribution of displacement fields. These requirements are named as C_z^0-requirements by Carrera [1]. Finally, the coupling between the in-plane and out-of-plane strain components has to be considered. In the present work, a refined model based on the Jacobi expansion is used for the modelling of multilayered one-dimensional (1D) beams and two-dimensional (2D) plates and shells structures.

When dealing with 1D structures, Euler-Bernoulli Beam Model (EBBM) [2] and the Timoshenko Beam Model (TBM) [3] are the classic models. In the first one, however, shear strain components are considered null, while in the second they are constant over the cross-section. When thin-walled and layered components are studied, higher-phenomena may appear within the structure, due to relevant deformation over the cross-section. In this case, it is necessary to adopt more refined theories, as described in the influential book by Novozhilov [4]. The works of Kapania and Raciti [5, 6] and Carrera *et al.* [7] give comprehensive reviews for 1D theories. Warping functions, which succeeded in capturing the deformations of the beam cross-section, were proposed by Vlasov [8]. Many scholars, as Ambrosini, Riera *et al.* [9], Mechab, Meiche et al. [10] and Friberg [11], adopted these functions for the analysis of thin-walled structures. Moreover, Schardt [12] suggested the so-called Generalized Beam Theory (GBT) which expresses the displacement field as a linear combination of cross-sectional deformation modes.

Concerning the 2D plate and shell theories, Kirchhoff-Love theory [13, 14] and First Shear Deformation Theory (FSDT), based on the works by Reissner [15] and Mindlin [16] are the 2D counterpart of EBBM and TBM, respectively. Classical Lamination Theory (CLT) [17] is the extension of Kirchoff-Love for laminated structures, and it neglects the out-of-plane strains. Consequently, some issues occured during the practical stages of the research. FSDT, which gives better results, considers shear strain components as a constant, and is used in commercial software tools. As classical theories are affected by some drawbacks, several refined plate Finite Elements (FEs) have recently been developed, as proposed by Reddy and Robbins Jr. [18] and Carrera [19]. When dealing with laminates, two approaches can be used: Equivalent Single Layer (ESL) and Layer-Wise (LW) models. In the first one, the number of unknowns are not affected by the number of layers, while in the second one, they are dependent on the number of layers (see Carrera [20]). Clearly, Layer-Wise models are adopted when a refined analysis is required, even though they demand a high computational cost. This influences the entire design process of the structural components. As this is a crucial point, most of the works suggested here adopt ESL theories.

Some higher-order theories with ESL approach are those developed by Reddy [21], the so-called zig-zag theories firstly proposed by Murakami [22] and the theories based on Reissner's Mixed Variational Theorem (RMVT) developed by Carrera [23]. Furthermore, Rammerstorfer, Dorninger, *et al.* [24], Reddy [25], Mawenya and Davies [26], and Noor and Burton [27] developed FE implementations using LW theories. Carrera [28] also proposed a unified formulation for 2D plate and shells using the Principle of Virtual Displacements or RMVT with ESL and LW approaches.

For beam, plate and shell modelling, refined theories differ from classical ones by using higher-order polynomials, e.g. Taylor polynomials (see Carrera *et al.* [29]), zig-zag theories by the same authors [30] and Lagrange expansions (see Pagani *et al.* [31]). In the present work, refined beam, plate and shell models are built using Jacobi polynomials. Jacobi expansions ([32, 33] consist of orthogonal polynomials, which can be derived from a recurrence relation. Jacobi polynomials are used in several numerical applications. Guo *et al.* [34] used generalized

Jacobi functions to resolve partial differential equations, while Abd-Elhameed [35] proposed an algorithm for solving sixth-order boundary value problems with the aid of the Galerkin method. Some papers on structural applications build hierarchical functions using integrated Jacobi polynomials (the interested reader can refer to Beuchler and Schöberl [36]). Jacobi polynomials are adopted as shape functions in FE elements and as expansions to generate structural theories. Szabo, *et al.* [37] proposed a h-p version of FE using hierarchical expansions derived from Legendre polynomials for beam, plate and solid. Beuchler and Pillwein [38] showed the efficiency of tetrahedral FEM for higher polynomial degrees. Fuentes *et al.* [39] suggested a similar FE method based on shifted Jacobi polynomials. They introduced several shapes for beam, plate and solid elements. Adopting general Jacobi polynomials, the Legendre case can be derived as a particular case of Jacobi polynomials. Li *et al.* [40] compared Legendre and Lagrange shape functions for 2D plate elements. Finally, Alanbay *et al.* [41] demonstrated the computational efficiency to calculate free vibration frequencies when weighted orthogonal Jacobi polynomials and Ritz method are adopted in plate simulations. Pagani *et al.* [42] used Legendre for 2D cross-section in beam formulation, while Carrera *et al.* [43] studied anisotropic plates by means of hierarchical 1D expansions constructed with Chebyshev polynomials. Finally, Carrera and Valvano [44] analysed composite structures with embedded piezoelectric sheets through ESL/LW approach with Legendre polynomials. This paper proposes hierarchical expansions built using Jacobi polynomials in the framework of CUF. This formulation is versatile since it can be used to derive beam, plate and shell models and the governing equations are invariant from the adopted theory of structure. In fact, type and order of expansion, together with the chosen approach, are the input for building a structural model. The formulation also makes it possible to use weak formulations for providing numerical solutions. In the present work, Lagrange polynomials have been chosen as shape functions of Finite Element Method (FEM).

This paper is structured as follows: Section 2 introduces the hierarchical Jacobi expansion, and in Section 3 the unified formulation and the adopted FEM are proposed. Furthermore, an explanation of is provided. In Section 4 significant results are presented. Finally, the main conclusions of this work are drawn in Section 5.

2 Hierarchical Jacobi polynomials for composite structures

In this paper, theories of structures based on Jacobi polynomials are considered. Differently from the Lagrange polynomials (see Pagani *et al.* [31]), where some selected points are used to generate the functions, they are formulated using recurrence relations, as done for Legendre polynomials. The relation describing the orthogonal Jacobi polynomials is expressed in the following

$$P_n^{(\gamma,\theta)}(\zeta) = (A_n\zeta + B_n)\, P_{n-1}^{(\gamma,\theta)}(\zeta) - C_n P_{n-2}^{(\gamma,\theta)}(\zeta) \tag{1}$$

where γ and θ are two parameters and n is the order of the polynomial. The relation is calculated in $\zeta = [-1, +1]$. The initial values are $P_0^{(\gamma,\theta)}(\zeta) = 1$ and $P_1^{(\gamma,\theta)}(\zeta) = A_0\zeta + B_0$. The parameters A_n, B_n and C_n are presented as follows

$$A_n = \frac{(2n + \gamma + \theta + 1)(2n + \gamma + \theta + 2)}{2(n + 1)(n + \gamma + \theta + 1)} \tag{2}$$

$$B_n = \frac{(\gamma^2 - \theta^2)(2n + \gamma + \theta + 1)}{2(n + 1)(n + \gamma + \theta + 1)(2n + \gamma + \theta)} \tag{3}$$

$$C_n = \frac{(n+\gamma)(n+\theta)(2n+\gamma+\theta+2)}{(n+1)(n+\gamma+\theta+1)(2n+\gamma+\theta)} \tag{4}$$

Other popular polynomials can be devised, by opportunely choosing values of the parameters γ and θ. For instance, Legendre polynomials are given by $\gamma = 0$ and $\theta = 0$ (see Fig. 1 (a) for the first five orders), while the First Kind of Chebyshev Polynomials (see Fig. 1 (b)) are given by the following formula

$$T_n(\zeta) = \frac{P_n^{\left(-\frac{1}{2},-\frac{1}{2}\right)}(\zeta)}{P_n^{\left(-\frac{1}{2},-\frac{1}{2}\right)}(1)} \tag{5}$$
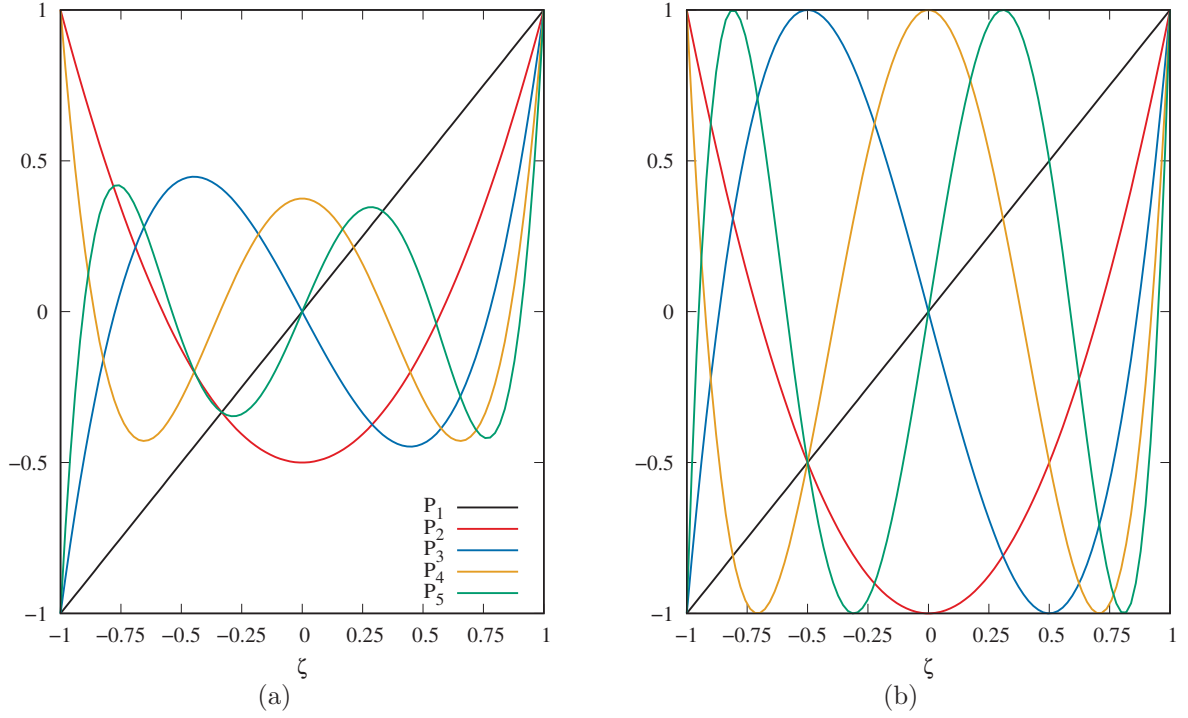

Figure 1: Legendre Polynomials (a) and First Kind of Chebyshev Polynomials (b) up to the fifth order.

2.1 Hierarchical Jacobi Expansion for plates and shells

Jacobi polynomials are used to build hierarchical functions, exploiting the fact that orthogonal polynomials are obtained using Eq. 1. For the 2D plates and shells, they are adopted as expansion functions with the procedure described in [37]. The expansion functions can be adopted for both the ESL and LW approaches in the CUF framework, described in Section 3. Fig. 2 shows a illustration of two-layer plate and shell cross-sections, where each layer is indicated by letter k. Figs. 2 (a,c) depict a ESL approach, where a single element is adopted along the cross-section, while Figs. 2 (b,d) show a discretization where one element is used for each layer.
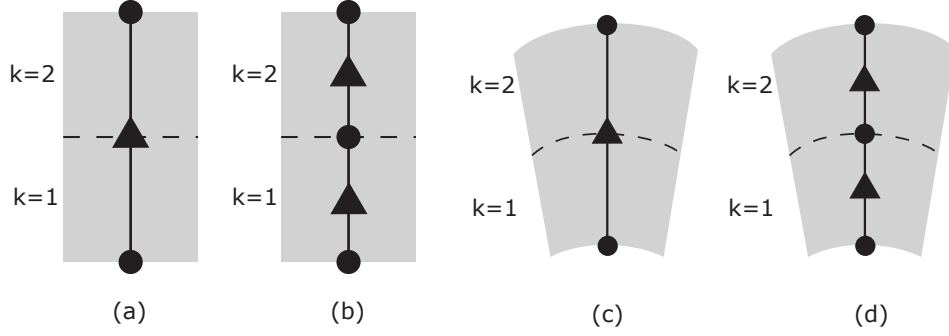
4

Figure 2: Hierarchical Jacobi Expansions for plate with ESL approach (a) and LW approach (b), and shell with ESL approach (c) and LW approach (d). ● represents an edge expansion, whereas ▲ is an inner expansion.

The set for hierarchic functions is given by

$$
\begin{aligned}
F_1(\zeta) &= \frac{1}{2}(1-\zeta) \\
F_2(\zeta) &= \frac{1}{2}(1+\zeta) \\
F_i(\zeta) &= \phi_{i-1}(\zeta), \quad i = 3, 4, ..., n+1
\end{aligned}
\tag{6}
$$

with

$$
\phi_j(\zeta) = (1-\zeta)(1+\zeta)P_{j-2}^{\gamma,\theta}(\zeta), \quad j = 2, 3, ..., n
\tag{7}
$$

The first two functions $F_1(\zeta)$, $F_2(\zeta)$ are the vertex expansions. Given the following property

$$
F_i(-1) = F_i(1) = 0, \quad i \geq 3
\tag{8}
$$

the functions $F_i(\zeta), i = 3, 4, ...$ are called bubble functions or edge expansions. The bubble functions for two different sets of parameters γ and θ are shown in Figs. 3 (a) and 3 (b) for the cases $\gamma = 1.5, \theta = -0.5$ and $\gamma = 0, \theta = 0$ (i.e. Legendre), respectively. [1]

2.2 Hierarchical Jacobi Expansion for beams

In this case, vertex, edge and internal polynomials are used as interpolation functions over the domain. When dealing with laminated structures, ESL and LW approaches, described in Section 3, can be exploited using the presented Jacobi polynomials. Figure 4 shows a beam cross-section, and each layer is indicated by letter k. The ESL technique is depicted in Fig. 4 and a single polynomial is employed for the whole cross-section, including the two layers, whereas a dedicated Jacobi polynomial is reserved for each layer in the LW procedure, shown in Fig. 4. A similar procedure is described in [43].

---

[1]In the literature (see [37] and [43]), the following bubble expression (or multiplied by a pre-factor) are used for Legendre and Chebyshev of the First Kind

$$
\phi_j^*(\zeta) = \int_{-1}^{\zeta} P_{j-1}^{\gamma,\theta} d\zeta, \quad j = 2, 3, ..., n
$$

but this procedure does not guarantee the condition in Eq. (7) for every choices of γ, θ and n.
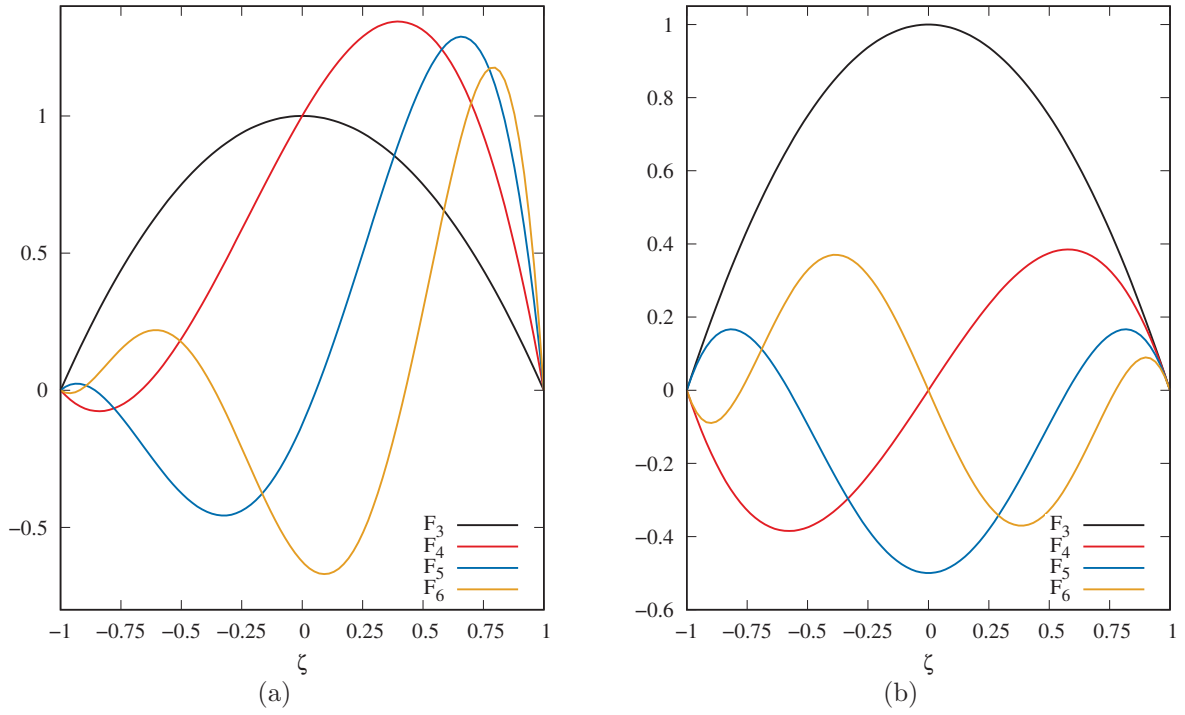
Figure 3: Edge expansion up to the fifth order with $\gamma = 1.5$, $\theta = -0.5$ (a) and $\gamma = 0$, $\theta = 0$ (b).
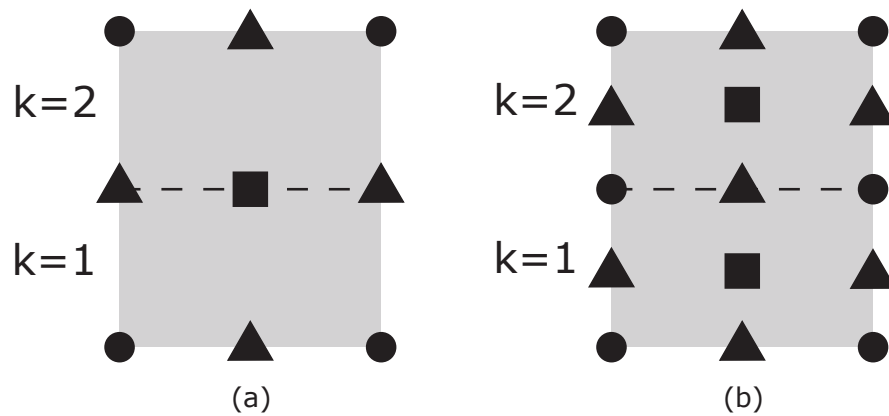

Figure 4: Hierarchical Jacobi Expansions for beam with ESL approach (a) and LW approach (b). ● represents a vertex expansion, whereas ▲ is an edge expansions and ■ indicates an internal expansions.
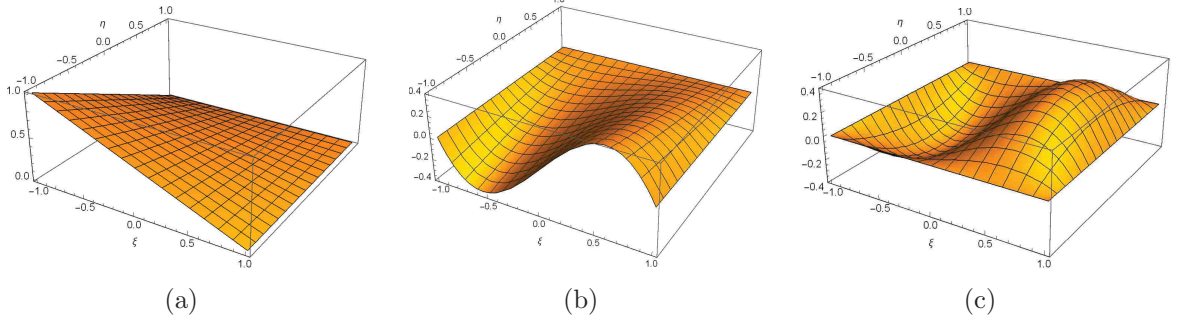
Figure 5: Vertex expansions (a), edge expansion (b) and internal expansion (c) for two-dimensional case with $\gamma = 0$, $\theta = 0$.

Vertex expansions The vertex modes correspond to the first-order, quadrilateral Lagrange polynomials:

$$F_\tau(\xi, \eta) = \frac{1}{4}(1 - \xi_\tau \xi)(1 - \eta_\tau \eta), \quad \tau = 1, 2, 3, 4 \tag{9}$$

where ξ and η vary above the domain between -1 and +1, and ξ_τ and η_τ represent the vertex coordinates in the natural plane. In Fig. 5 (a), F_1 vertex expansion is shown.

Edge expansions The edge modes are defined for $p \geq 2$ in the natural plane as follows

$$
\begin{aligned}
F_\tau(\xi, \eta) &= \frac{1}{2}(1 - \eta)\, \phi_p(\xi), \quad \tau = 5, 9, 13, 18, ... \\
F_\tau(\xi, \eta) &= \frac{1}{2}(1 + \xi)\, \phi_p(\eta), \quad \tau = 6, 10, 14, 19, ... \\
F_\tau(\xi, \eta) &= \frac{1}{2}(1 + \eta)\, \phi_p(\xi), \quad \tau = 7, 11, 15, 20, ... \\
F_\tau(\xi, \eta) &= \frac{1}{2}(1 - \xi)\, \phi_p(\eta), \quad \tau = 8, 12, 16, 21, ...
\end{aligned}
\tag{10}
$$

where p represents the polynomial degree of the bubble function. In Fig. 5 (b), F_9 edge expansion (linked to the third order of Jacobi polynomials) is displayed.

Internal expansions F_τ internal expansions are built by multiplying 1D edge modes. There are $(p - 2)(p - 3)/2$ internal polynomials for $p \geq 4$ and they vanish at all the edges of the quadrilateral. For instance, considering the set of fifth-order polynomials, it contains 3 internal expansions, which are

$$
\begin{aligned}
F_{22}(\xi, \eta) &= \phi_3(\xi)\phi_2(\eta), \quad 3 + 2 = 5 \\
F_{23}(\xi, \eta) &= \phi_2(\xi)\phi_3(\eta), \quad 2 + 3 = 5 \\
F_{17}(\xi, \eta) &= \phi_2(\xi)\phi_2(\eta), \quad 2 + 2 = 4
\end{aligned}
\tag{11}
$$

In Fig. 5 (c), F_{22} internal expansion (linked to the fifth order of Jacobi polynomials) is displayed.

7

3 Unified formulation for beams, plates and shells

3.1 Preliminaries and CUF assumptions

In this section, the Carrera Unified Formulation (CUF) is presented for beams, plates and shells. In the present work, hierarchical Jacobi polynomials are adopted as expansion functions.

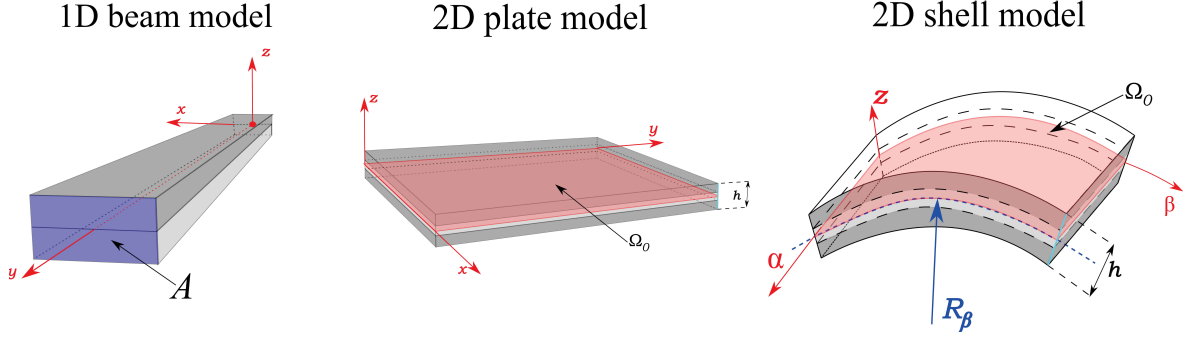Let us consider multilayered beam, plate and shell structures as shown in Fig. 6.

Figure 6: Generic multilayered beam, plate and shell models. For 1D model, y is the direction of the beam axis, and z is the thickness coordinate of the 2D models. A Cartesian reference system is employed for the 1D beam and 2D plate models (x, y, z), whereas a curvilinear system (α, β, z) is used for the 2D shell model.

The cross-section A of the 1D model lays on the $x - z$ plane of a Cartesian reference system. As a consequence, the beam axis is placed along the y direction and the 2D plate model uses the z coordinate for the thickness direction and the coordinates x and y indicate the in-plane mid-surface Ω_0. Finally, the shell uses a curvilinear reference frame (α, β, z) to account for the curvature, where α and β are the two in-plane directions. In this work, only single curvature shell structures (i.e cylindrical shells) are considered. The displacement vector for the models is introduced in the following

$$\mathbf{u}^k(x, y, z) = \left\{ \begin{array}{ccc} u_x^k & u_y^k & u_z^k \end{array} \right\}^T, \quad \mathbf{u}^k(\alpha, \beta, z) = \left\{ \begin{array}{ccc} u_\alpha^k & u_\beta^k & u_z^k \end{array} \right\}^T \tag{12}$$

where k indicates the layer. In the relations shown in Eq. (12), a Cartesian reference system is adopted for the former, and a curvilinear system for the latter. The stress, $\boldsymbol{\sigma}^k$, and strain, $\boldsymbol{\epsilon}^k$, vectors are expressed in vectorial form,

$$\boldsymbol{\sigma}^k = \left\{ \begin{array}{cccccc} \sigma_{xx}^k & \sigma_{yy}^k & \sigma_{zz}^k & \sigma_{xz}^k & \sigma_{yz}^k & \sigma_{xy}^k \end{array} \right\}^T, \quad \boldsymbol{\epsilon}^k = \left\{ \begin{array}{cccccc} \epsilon_{xx}^k & \epsilon_{yy}^k & \epsilon_{zz}^k & \epsilon_{xz}^k & \epsilon_{yz}^k & \epsilon_{xy}^k \end{array} \right\}^T$$

$$\boldsymbol{\sigma}^k = \left\{ \begin{array}{cccccc} \sigma_{\alpha\alpha}^k & \sigma_{\beta\beta}^k & \sigma_{zz}^k & \sigma_{\alpha z}^k & \sigma_{\beta z}^k & \sigma_{\alpha\beta}^k \end{array} \right\}^T, \quad \boldsymbol{\epsilon}^k = \left\{ \begin{array}{cccccc} \epsilon_{\alpha\alpha}^k & \epsilon_{\beta\beta}^k & \epsilon_{zz}^k & \epsilon_{\alpha z}^k & \epsilon_{\beta z}^k & \epsilon_{\alpha\beta}^k \end{array} \right\}^T \tag{13}$$

The displacement-strain relations are expressed as

$$\boldsymbol{\epsilon}^k = \mathbf{b}\mathbf{u}^k \tag{14}$$

where $\mathbf{b}$ is the matrix of differential operators. More informations can be found in Carrera *et al.* [45, 46].

As far as the constitutive relation is concerned, linear elastic orthotropic materials are considered in this work. Consequently, the constitutive relation reads as:

$$\boldsymbol{\sigma}^k = \mathbf{C}^k \boldsymbol{\epsilon}^k, \tag{15}$$

where $\mathbf{C}^k$ is the material elastic matrix, whose explicit form can be found in Bathe [47] and Hughes [48].

Within the framework of the CUF, the 3D displacement field $\mathbf{u}^k(x, y, z)$ of the 1D beam and 2D plate and $\mathbf{u}^k(\alpha, \beta, z)$ of 2D shell models can be expressed as a general expansion of the primary unknowns. The displacements can be conveniently written in the most general way for all the three formulations as follows

$$\mathbf{u}^k(x, y, z) = F_\tau^k \mathbf{u}_\tau^k \tag{16}$$

F_τ are the expansion functions of the *generalized* displacements $\mathbf{u}_\tau$, the Einstein convention

Formulation	3D Fields	CUF Expansion	
1D beam :	$\mathbf{u}^k(x, y, z)$	$F_\tau^k(x, z)$	$\mathbf{u}_\tau^k(y)$
2D plate :	$\mathbf{u}^k(x, y, z)$	$F_\tau^k(z)$	$\mathbf{u}_\tau^k(x, y)$
2D shell :	$\mathbf{u}^k(\alpha, \beta, z)$	$F_\tau^k(z)$	$\mathbf{u}_\tau^k(\alpha, \beta)$

Table 1: CUF formulation. τ is the repeated indexes with $\tau = 1, 2, ..., M$, while M denotes the order of expansion.

with the repeated index τ is assumed, M denotes the order of expansion. In Table 1, the independent variables are explicitly shown for each formulation.

3.2 Finite Element Approximation

The Finite Element Method (FEM) is adopted to discretise the generalized displacements $\mathbf{u}_\tau^k$. Thus, recalling equations described in Table 1, they are approximated as displayed in Table 2, where N_i stand for the shape functions, the repeated subscript i indicates summation, N_n

Formulation	3D Field	FEM+CUF Expansions		
1D beam :	$\mathbf{u}^k(x, y, z)$	$N_i(y)$	$F_\tau^k(x, z)$	$\mathbf{u}_{\tau i}^k$
2D plate :	$\mathbf{u}^k(x, y, z)$	$N_i(x, y)$	$F_\tau^k(z)$	$\mathbf{u}_{\tau i}^k$
2D shell :	$\mathbf{u}^k(\alpha, \beta, z)$	$N_i(\alpha, \beta)$	$F_\tau^k(z)$	$\mathbf{u}_{\tau i}^k$

Table 2: Finite element method. i is repeated index with $i = 1, 2, ..., N_n$, N_n is the number of the FE nodes per element.

is the number of the FE nodes per element and $\mathbf{u}_{\tau i}^k$ are the following vectors of the FE nodal parameters:

$$\mathbf{u}_{\tau i}^k = \left\{ u_{x_{\tau i}}^k \, u_{y_{\tau i}}^k \, u_{z_{\tau i}}^k \right\}^T \quad \mathbf{u}_{\tau i}^k = \left\{ u_{\alpha_{\tau i}}^k \, u_{\beta_{\tau i}}^k \, u_{z_{\tau i}}^k \right\}^T \tag{17}$$

In this work, when using formulation for beam, classical one-dimensional FEs with three-node(B3) and four-node (B4) are adopted, i.e. parabolic and cubic approximation along the y axis are assumed, respectively. For the 2D plate and shell formulations, classical 2D nine-node bi-quadratic FEs (Q9) is adopted for the shape function in the x, y and α, β planes, see Bathe [47] for more details. These shape functions have been chosen, since they have a faster convergence than linear (B2) and bi-linear (Q4) elements.

Formulation	Displacement	Virtual Displacement
1D beam :	$\mathbf{u}^k(x,y,z) = N_i(y)F_\tau^k(x,z)\mathbf{u}_{\tau i}^k$	$\delta\mathbf{u}^k(x,y,z) = N_j(y)F_s^k(x,z)\delta\mathbf{u}_{sj}^k$
2D plate :	$\mathbf{u}^k(x,y,z) = N_i(x,y)F_\tau^k(z)\mathbf{u}_{\tau i}^k$	$\delta\mathbf{u}^k(x,y,z) = N_j(x,y)F_s^k(z)\delta\mathbf{u}_{sj}^k$
2D shell :	$\mathbf{u}^k(\alpha,\beta,z) = N_i(\alpha,\beta)F_\tau^k(z)\delta\mathbf{u}_{\tau i}^k$	$\delta\mathbf{u}^k(\alpha,\beta,z) = N_j(\alpha,\beta)F_s^k(z)\delta\mathbf{u}_{sj}^k$

Table 3: Displacements and virtual displacements. τ and s are the repeated indexes with $\tau, s = 1, 2, ..., M$, while M denotes the order of expansion. i and j are repeated index with $i, j = 1, 2, ..., N_n$, N_n is the number of the FE nodes per element.

3.3 Governing equations and Finite Element Matrices

The Principle of Virtual Displacements (PVD) is used and it reads:

$$\int_{V_k} (\delta\boldsymbol{\epsilon}^T \boldsymbol{\sigma}) \mathrm{d}V_k \;\; = \;\; \delta L_e \tag{18}$$

where V_k is the integration domain and k is the considered mathematical layer. The left-hand side of the equation represents the variation of the internal work, while the right-hand side is the virtual variation of the external work. Since the real and the virtual systems are used in PVD, it is useful to show how the displacements are expressed and which indexes are used in the different systems (see Table 3). When an approach has to be introduced, LW has different functions for each layer k, whereas ESL uses the same functions for every layer k.
Substituting the geometrical relations (Eq. (14)), the constitutive equation (Eq. (15)), and applying the CUF (Table (1)) and the FEM (Table (2)), the following governing equations are obtained:

$$\delta\mathbf{q}_{sj}^k : \;\; \mathbf{K}^{kij\tau s}\, \mathbf{q}_{\tau i}^k = \mathbf{P}_{sj}^k \tag{19}$$

where $\mathbf{K}^{kij\tau s}$ is a 3×3 matrix, called fundamental nucleus (FN) of the mechanical stiffness matrix. The stiffness matrix of each layer k is obtained from the expansion of the FN on the indexes τ and s. On the other hand, $\mathbf{P}_{sj}^k$ is a 3×1 matrix, called fundamental nucleus of the external load (see [49, 46] for further details). Then, the matrices of each layer are assembled at the multi-layer level.

4 Numerical Results

In this section, results on displacements and stresses are displayed for four benchmarks. They are compared with reference solutions from the open literature (see Table 4 for a schematic representation). It is demonstrated that, given the polynomial order, the parameters γ and θ do not alter the results. Thence, there are no specifications in tables and figures. When the results are presented as LJn, it indicates Layer-Wise (Hierarchical) Jacobi and n is the polynomial order, whereas EJn stands for Equivalence Single Layer (Hierarchical) Jacobi. For the shear stresses results, the letter H indicates the use of Hooke's Law, and the letter I stands for stress recovery method. The tables report only stresses from Hooke's Law.

4.1 Convergence characteristics and shear locking treatment for the proposed elements

Here, numerical issues for thin structures are analysed. The convergence of transverse displacement is studied for beams, plates and shells. In order to investigate the shear locking
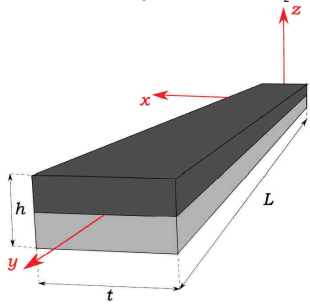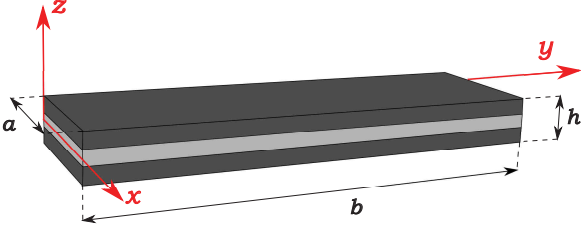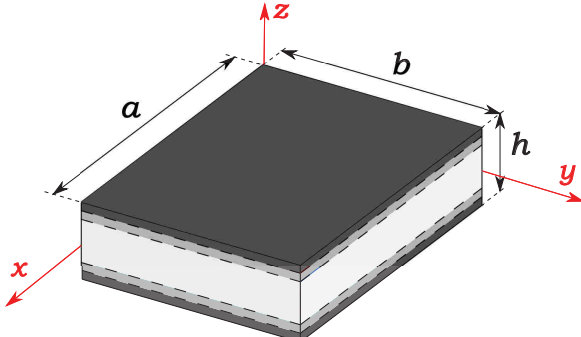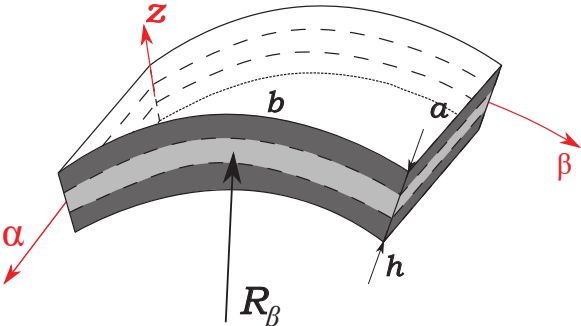
B1: Two-layer Beam [50]	**B2: Three-layer plate [51]**
$L/h = 20, 200$ and $h/t = 0.5$ Cantilever beam loaded by a uniform pressure at the top position towards negative z-axis. $P = 1000$Pa	$b/h = 4, 1000$ and $a = 1$ Simply supported, loaded with a transverse sinusoidal pressure $p = P_z \sin\left(\frac{\pi x}{b}\right)$ at the top position with $P_z = 1Pa$
B3: Five-layer sandwich plate [52, 53]	**B4: Three-layer shell [54, 28]**
$a/h = 100$, $a = b$, $h_3 = 8mm$, $h_1 = h_2 = h_4 = h_5 = 0.5mm$ Simply supported, loaded with a transverse sinusoidal pressure $p = P_z \sin\left(\frac{\pi x}{a}\right)\sin\left(\frac{\pi x}{a}\right)$ at the top position with $P_z = 1Pa$	$R_\beta/b = \pi/3$, $R_\beta/h = 4, 10, 1000$ and $a = 1$ Simply supported, loaded with a transverse sinusoidal pressure $p = P_z \sin\left(\frac{\pi x}{b}\right)$ at the top position with $P_z = 1Pa$

Table 4: Geometrical properties of the four Benchmarks.

problem, very thin structures are taken into account. Four types of integration techniques are compared, namely, Full scheme (F), Reduced integration scheme (R)(see Zienkiewicz *et al.* [55]), Selective integration scheme (S)(see Kavanagh *et al.* [56]) and Mixed Interpolation Tensorial Components (MITC)(see Bucalem *et al.* [57]). Finally, for extended reviews, see [46] and Carrera *et al.* [58] . The first case is the two-layer composite beam presented in Carrera *et al.* [50]. Parabolic (B3) FEM elements are used, whereas LJ5 and EJ5 theories along the cross-section are adopted for composite and bimetallic beams with $L/h = 200$. Fig. 7 show how shear locking phenomenon is dependent only by the FEM discretization, while structural theories is not affected by this numerical phenomenon. A faster convergence for LJ5 is given because it has more degrees of freedom than EJ5. Furthermore, thin three-layered plate ($b/h = 1000$) and shell ($R_\beta/h = 1000$) are considered, respectively from Pagano [51] and Ren [54]. Biquadratic (Q9) FEM elements are used, whereas LJ5 and EJ5 theories along the cross-section are employed for both structures. For the sake of conciseness, only results with LJ5 theory are shown in Fig. 8, since EJ5 theory gives very similar results, as already demonstrated for the beam case. Finally, the integration techniques are able to resolve the numerical issues for beam, plate and shell formulations.
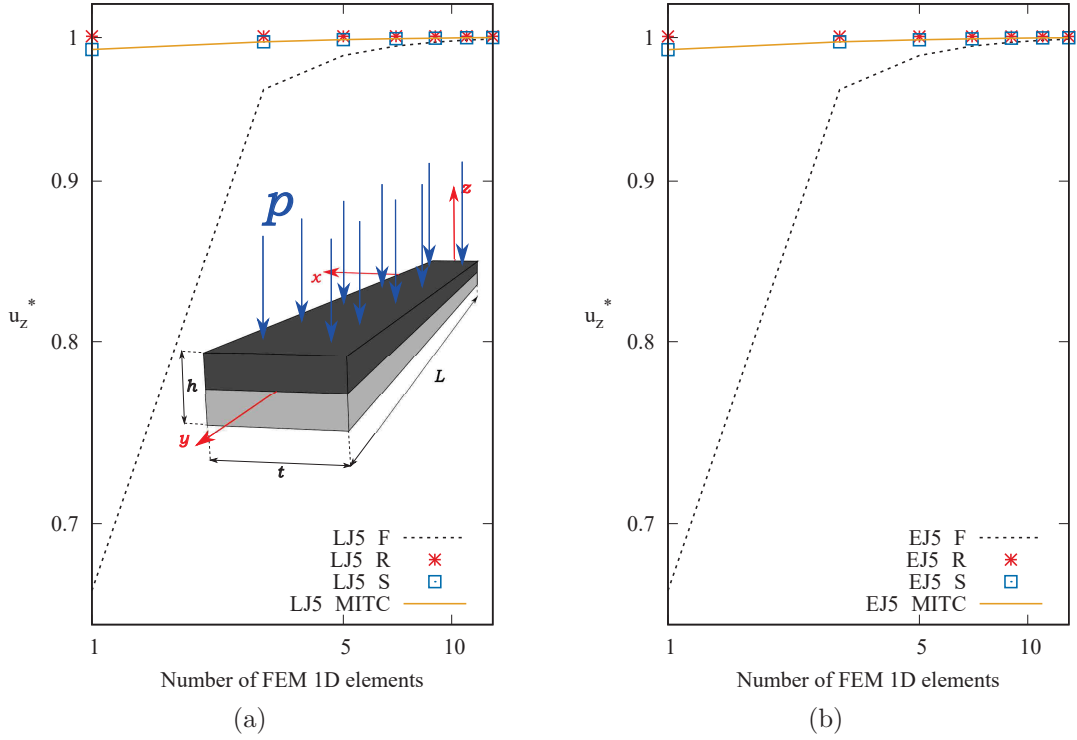
Figure 7: Study of convergence of transverse displacements in $[0, L, 0]$ for clamped two-layer composite beam with 1D formulation using LJ5 (a) and EJ5 (b) theories along the cross-section. Results are normalized by LJ5-MITC.
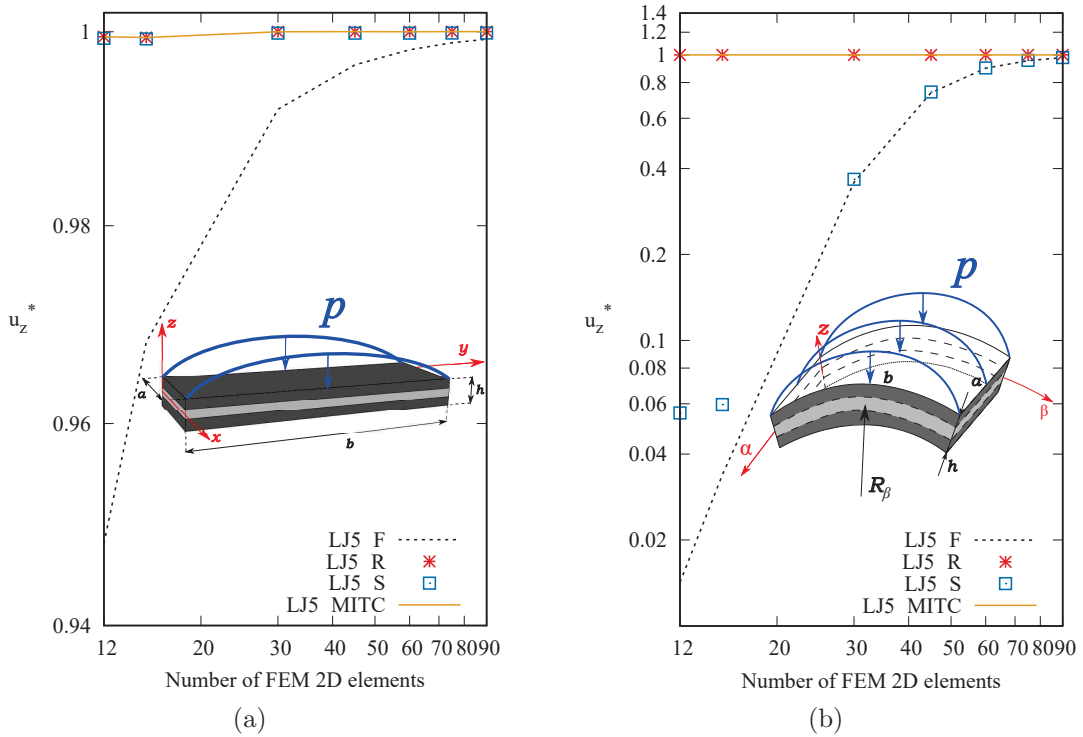

Figure 8: Study of convergence of transverse displacements in $[a/2, b/2, 0]$ section for three-layer composite plate with 2D formulation (a) and three-layer composite shell with shell formulation (b) using LJ5 theories along the cross-section. Results are normalized by LJ5-MITC.

12

4.2 B1: Two-layer beam

As first assessment, a two-layer composite and a bimetallic beam are considered. The analysis was firstly proposed by Carrera *et al.* [50]. Regarding the cross-ply beam, good results can be achieved for the transverse displacements and the in-plane stresses as displayed in Table 5 and Fig. 9, while there are greater differences for the shear stresses calculated through the Hooke's Law (see Table 5 and Fig. 10). Excellent results can be obtained if the shear stresses are calculated through the integration of indefinite equilibrium equations, i.e. the stress recovery technique, and remarkable improvements are obtained also for lesser refined theories. Considering the bimetallic structure, again the displacements and the in-plane stresses are in general well captured (see Table 6). In this case, it is particularly difficult to obtain a similar distribution of the shear stresses (as illustrated in Table 6 and Fig. 10) because of transverse anisotropy of the material properties; i.e. E_3 is different along the z direction, while it is constant for the composite. Indeed, a big hiatus is observed at the interface layer for ESL theory. Adopting the stress recovery method can resolve these problems.

Model	$-u_z \times 10^3 mm$	$\sigma_{yy} \times 10^3 MPa$	$\sigma_{yz} \times 10^3 MPa$	DOF
LW[50]	5.263	90.33	23.00	1848
Present Analysis(Layer-Wise)				
LJ1	5.220	90.93	16.35	396
LJ2	5.246	91.04	16.35	858
LJ3	5.263	90.40	23.00	1320
LJ4	5.263	90.27	23.02	1914
LJ5	5.263	90.30	23.01	2640
Present Analysis(Equivalent Single Layer)				
EBBM	5.140	92.96	—	66
TBM	5.265	92.38	10.02	110
EJ1	5.147	95.91	10.07	264
EJ2	5.233	91.04	16.35	528
EJ3	5.240	91.55	14.76	792
EJ4	5.256	90.60	20.34	1122
EJ5	5.260	90.13	22.27	1518

Table 5: Transverse displacement,in-plane and shear stresses of two-layer composite beam with 1D formulation. $-u_z$ calculated in $[0, L, 0]$, σ_{yy} calculated in $[0, L/2, 0.05m]$ and σ_{yz} calculated in $[0, L/2, -0.025m]$.

4.3 B2: Three-layer composite plate

For the second benchmark a thick plate ($b/h = 4$) is considered. The analysis was originally proposed by Pagano [51] and further investigated by Carrera [59]. Transverse displacements are compared in Table 7. Classical models are not able to approach the reference solution, while the J ESL models can improve the results. Once again, LW models lead to the most accurate results. Similar conclusions can be drawn when looking at the in-plane stresses (see Table 7 and Fig. 13 (a) and Fig. 14 (a)) and transverse stresses as one can see in Figs. 13 (b) and 14 (b). Shear stresses are calculated through constitutive relation. Some drawbacks are found for the classical and ESL models, especially because the continuity and zero condition

Model	$-u_z \times 10^3 mm$	$\sigma_{yy} \times 10^3 MPa$	$\sigma_{yz} \times 10^3 MPa$	DOF
LW[50]	0.2008	234.8	11.58	5124
Present Analysis(Layer-Wise)				
LJ1	0.1808	237.5	12.16	1098
LJ2	0.2008	234.7	11.74	2379
LJ3	0.2009	234.7	12.22	3660
LJ4	0.2010	234.9	13.09	5307
LJ5	0.2010	234.8	12.95	7320
Present Analysis(Equivalent Single Layer)				
EBBM	0.2025	234.4	—	183
TBM	0.2029	234.8	14.80	305
EJ1	0.1629	234.8	14.79	732
EJ2	0.2006	235.0	11.35	1464
EJ3	0.2008	234.7	15.49	2196
EJ4	0.2009	234.8	15.64	3111
EJ5	0.2010	234.9	13.73	4209

Table 6: Transverse displacement,in-plane and shear stresses of bimetallic beam with 1D formulation. $-u_z$ calculated in $[0, L, 0]$, σ_{yy} calculated in $[0, L/2, 0.05m]$ and σ_{yz} calculated in $[0, L/2, -0.01249m]$.
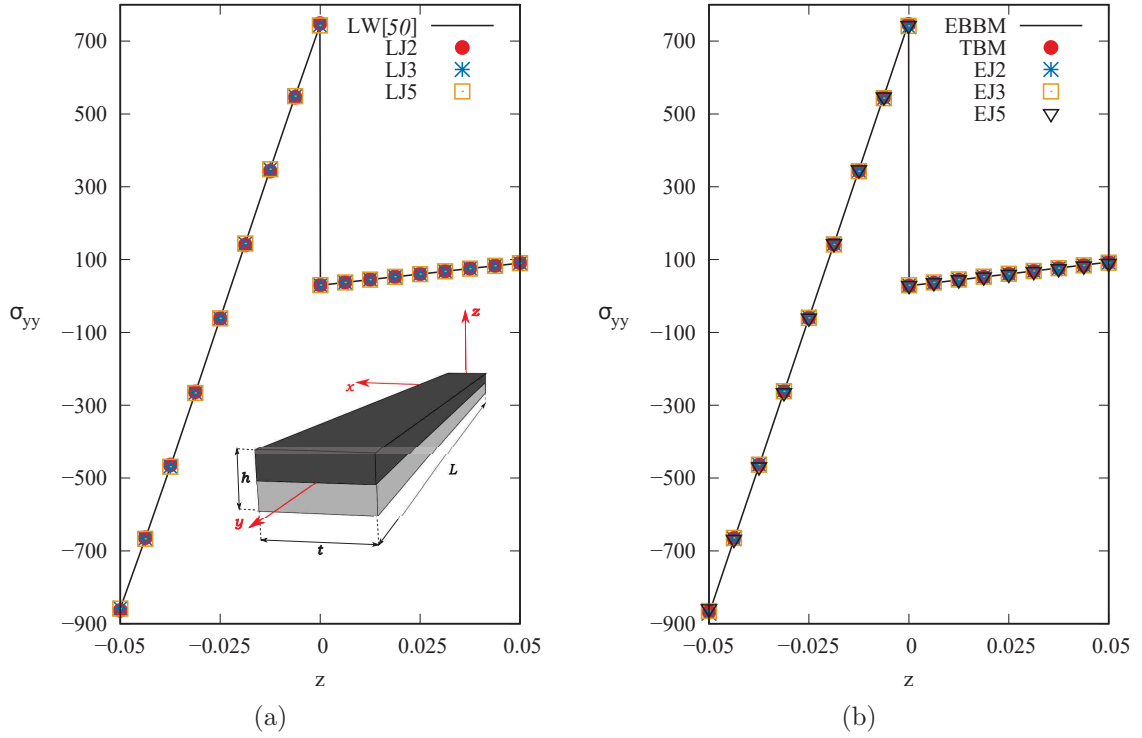

Figure 9: In-plane stresses calculated in $[0, L/2, z]$ of two-layer composite beam with 1D formulation for LW (a) and ESL (b) models.
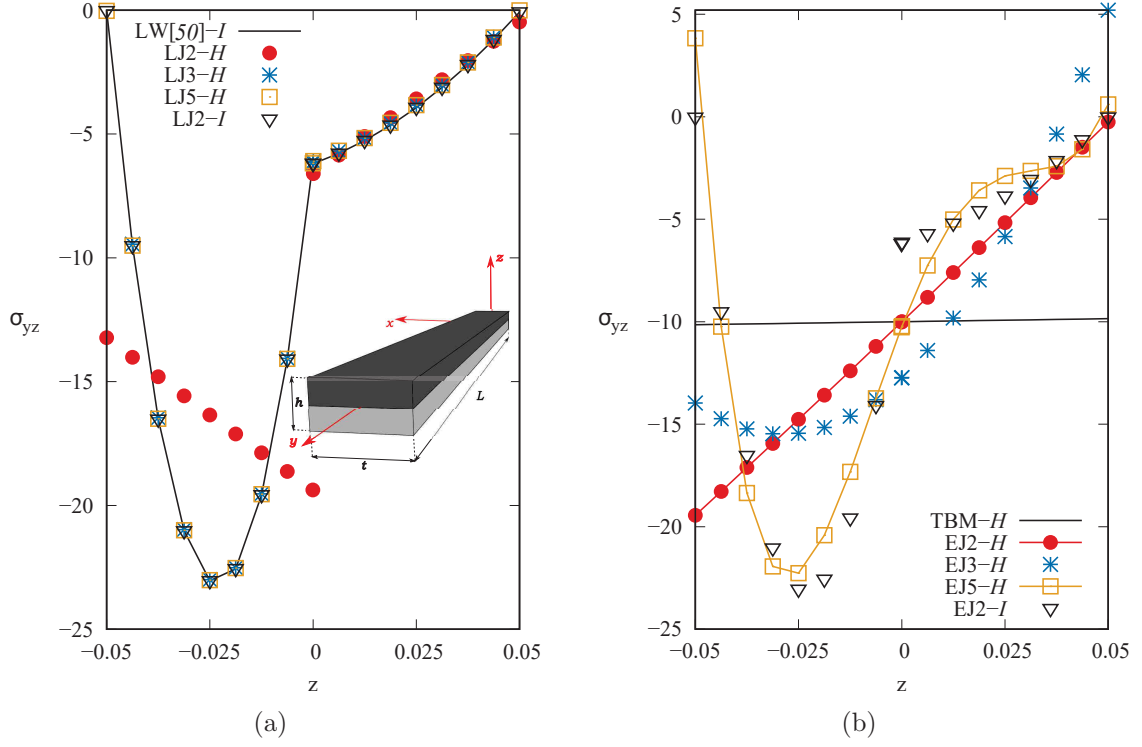
Figure 10: Shear stresses calculated in $[0, L/2, z]$ of two-layer composite beam with 1D formulation for LW (a) and ESL (b) models.
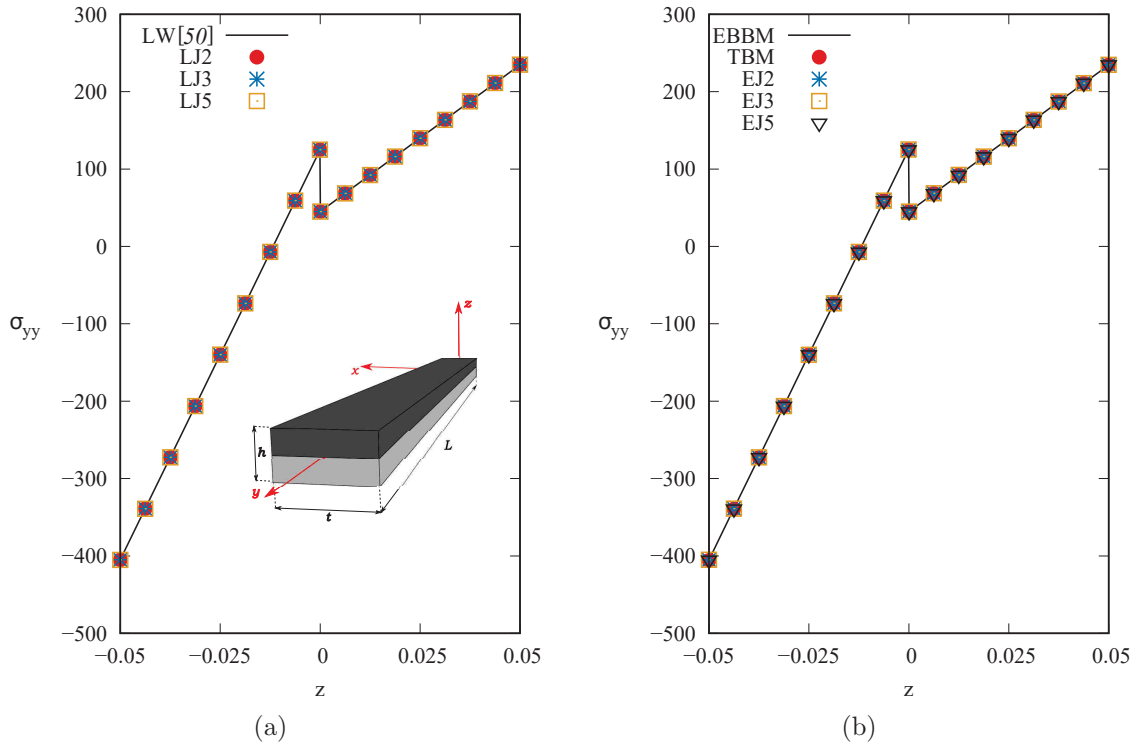

Figure 11: In-plane stresses calculated in $[0, L/2, z]$ of bimetallic beam with 1D formulation for LW (a) and ESL (b) models.
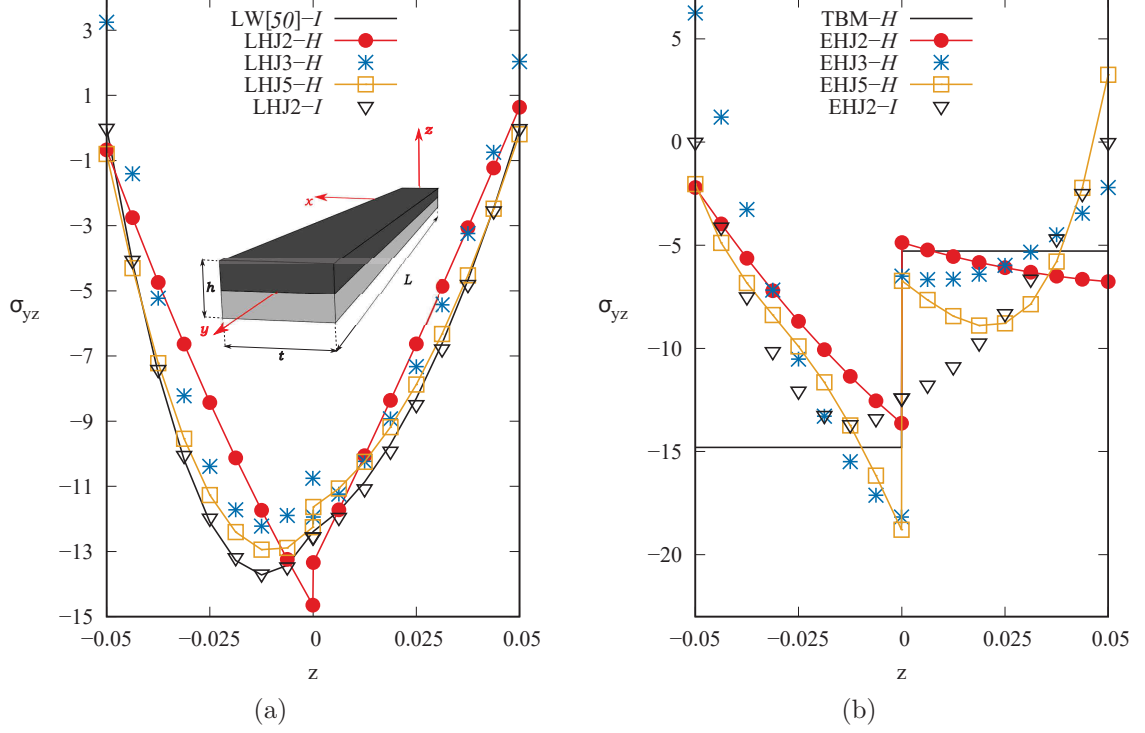
Figure 12: Shear stresses calculated in $[0, L/2, z]$ of bimetallic beam with 1D formulation for LW (a) and ESL (b) models.

at the low and top positions are not respected (see Table 7 and Fig. 15 (b)). LW models, except for the LJ1 and LJ2, can overwhelm these problems almost perfectly (see Table 7 and Fig. 15 (a)). Secondly, the shear stresses are obtained adopting the stress recovery method, which improves the results. However, some significant differences persist for the ESL models.

4.4   B3: Five-layer composite sandwich plate

A thin sandwich plate $(a/h = 100)$ is presented as the third benchmark. This study case is taken from Pagani, Valvano *et al.* [52] and Petrolo and Lamberti [53]. Considering the transverse displacements, classical and ESL models are not able to approach the LW reference solution and to have a similar trend, while the LW theories reproduce it (see Table 8 and Fig. 16) very accurately. The in-plane stresses, as displayed in Table 8 and Fig. 17, are well reproduced by every theory. Several problems, instead, arise from the calculations of the shear stresses, using only the Hooke's Law. The theories with lesser degrees of freedom are very dissimilar from the reference and LW solutions (which are very close to the first), as it is usual for plates with great anisotropies along the transverse direction (see Table 8 and Fig. 18). In this case a LW approach is mandatory to obtain good results for shear stresses.

4.5   B4: Three-layer composite shell

The last benchmark deals with a cylindrical shell, considering two different thickness $R_\beta/h = 4$ and $R_\beta/h = 10$. The analysis was originally proposed by Ren [54] and further investigated by Carrera [28]. Firstly, the thick shell $R_\beta/h = 4$ is analysed. Regarding the transverse displacements (see Table 9), classical models are not suitable to calculate it, while the ESL

Model	$\overline{u}_z$	$\overline{\sigma}_{xx}$	$\overline{\sigma}_{xz}$	DOF
Exact[51]	2.887	1.176	0.358	—
Present Analysis(Layer-Wise)				
LJ1	2.881	1.003	0.361	2604
LJ2	2.864	1.155	0.355	4557
LJ3	2.887	1.173	0.359	6510
LJ4	2.887	1.173	0.359	8463
LJ5	2.887	1.173	0.359	9765
Present Analysis(Equivalent Single Layer)				
CLT	0.511	0.629	—	651
FSDT	2.093	0.633	0.160	1085
EJ1	2.092	0.626	0.160	1302
EJ2	2.074	0.651	0.159	1953
EJ3	2.687	1.136	0.285	2604
EJ4	2.685	1.134	0.285	3255
EJ5	2.741	1.134	0.324	3906

Table 7: Transverse displacement, in-plane and shear stresses of three-layer composite plate under sinusoidal pressure with 2D formulation. $\overline{u}_z$ calculated in $[a/2, b/2, 0]$, $\overline{\sigma}_{xx}$ calculated in $[a/2, b/2, h/2]$, $\overline{\sigma}_{xz}$ calculated in $[a/2, 0, 0]$.
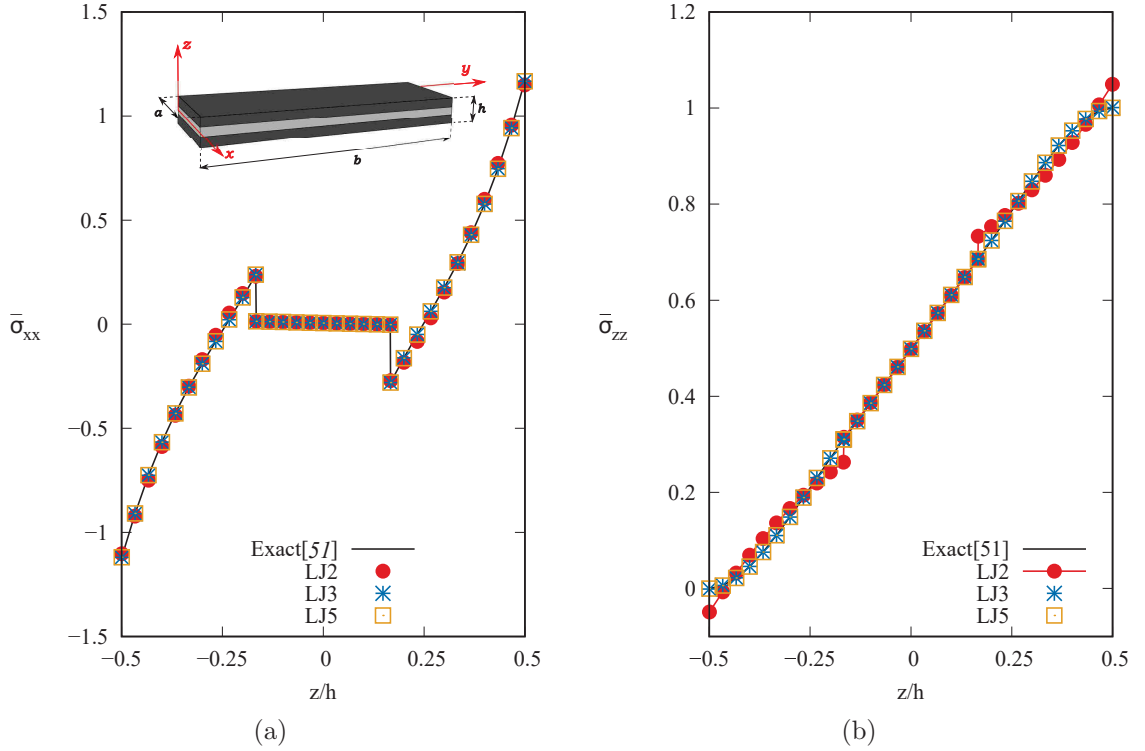

Figure 13: In-plane(a) and transverse (b) stresses in $[a/2, b/2, z]$ for three-layer composite plate with 2D formulation for LW models.
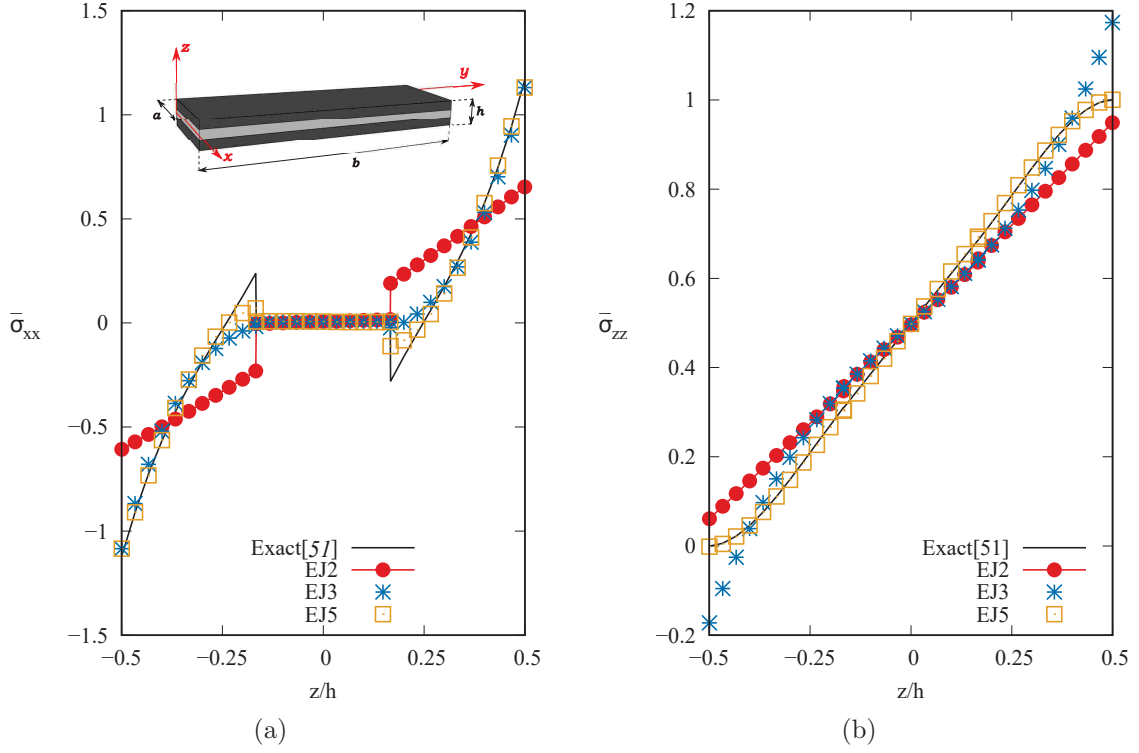
Figure 14: In-plane(a) and transverse (b) stresses in $[a/2, b/2, z]$ for three-layer composite plate with 2D formulation for ESL models.
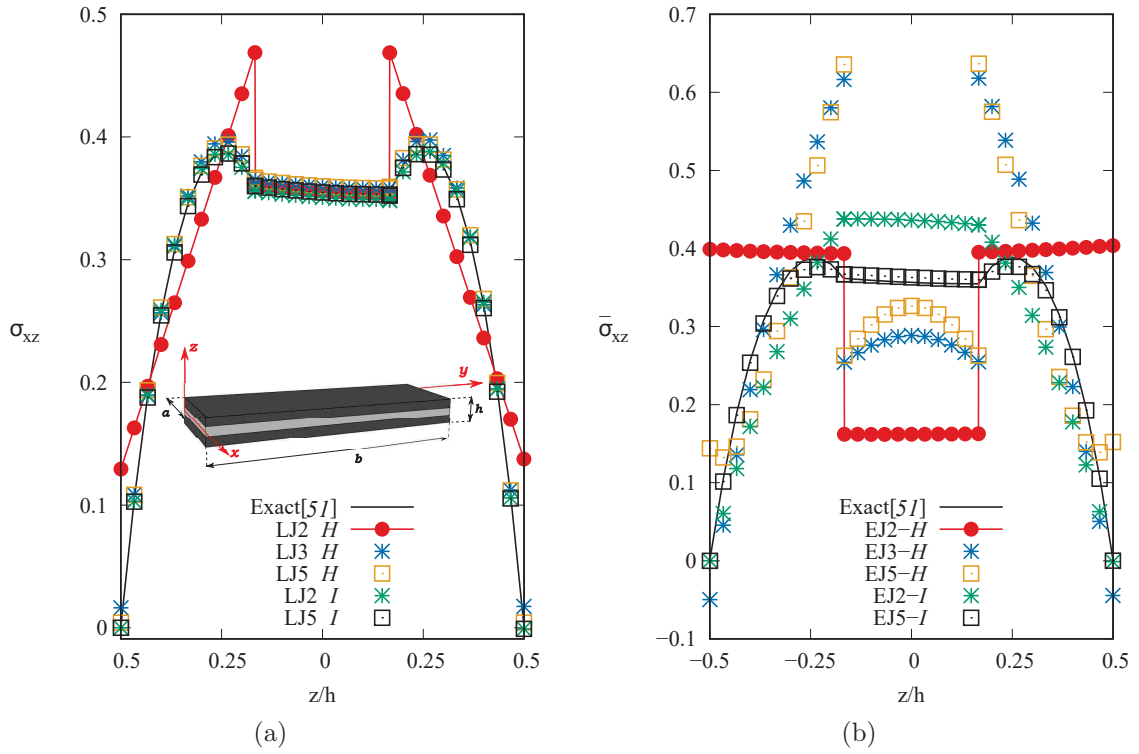

Figure 15: Shear stresses in $[a/2, 0, z]$ for three-layer composite plate with 2D formulation for LW (a) and ESL models (b).

Model	$\overline{u}_z$	$\overline{\sigma}_{xx}$	$\overline{\sigma}_{xz}$	DOF
LW[52]	3.1167	-0.7819	0.1825	27783
ESL[52]	3.0220	-0.7795	0.0917	6615
Present Analysis(Layer-Wise)				
LJ1	3.1241	-0.7762	0.1823	44652
LJ2	3.1167	-0.7762	0.1859	78141
LJ3	3.1167	-0.7762	0.1825	111630
LJ4	3.1167	-0.7762	0.1825	145119
LJ5	3.1167	-0.7762	0.1825	178608
Present Analysis(Equivalent Single Layer)				
CLT	2.9363	-0.7697	—	11163
FSDT	2.9429	-0.8004	0.0048	18605
EJ1	2.8218	-0.7674	0.0048	22326
EJ2	2.9429	-0.7713	0.0048	33489
EJ3	3.0222	-0.7739	0.0929	44652
EJ4	3.0222	-0.7738	0.0929	55815
EJ5	3.1088	-0.7690	0.2306	66978

Table 8: Transverse displacement, in-plane and shear stresses of the five-layer composite sandwich plate with 2D formulation. $\overline{u}_z$ calculated in $[a/2, a/2, +h/2]$, $\overline{\sigma}_{xx}$ calculated in $[a/2, a/2, -h/2]$, $\overline{\sigma}_{xz}$ calculated in $[0, a/2, 0]$.
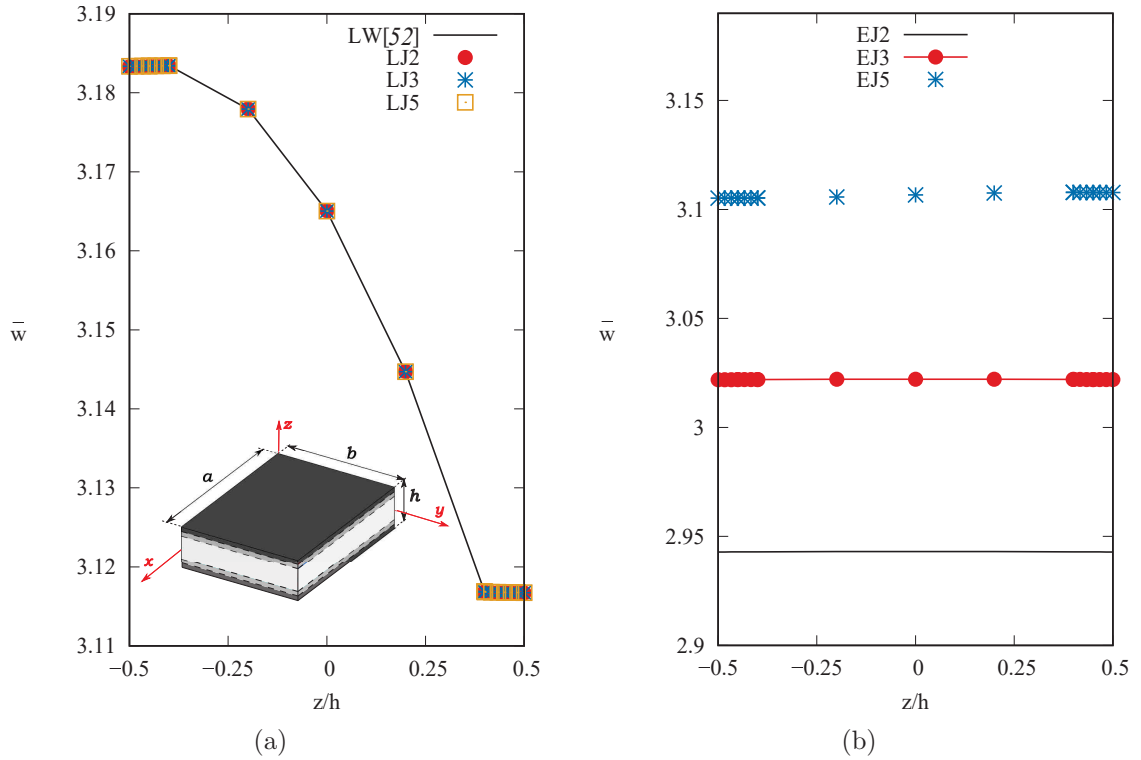

Figure 16: Transverse displacement in $[a/2, a/2, z]$ of five-layer composite sandwich with 2D formulation for LW (a) and ESL (b) models.
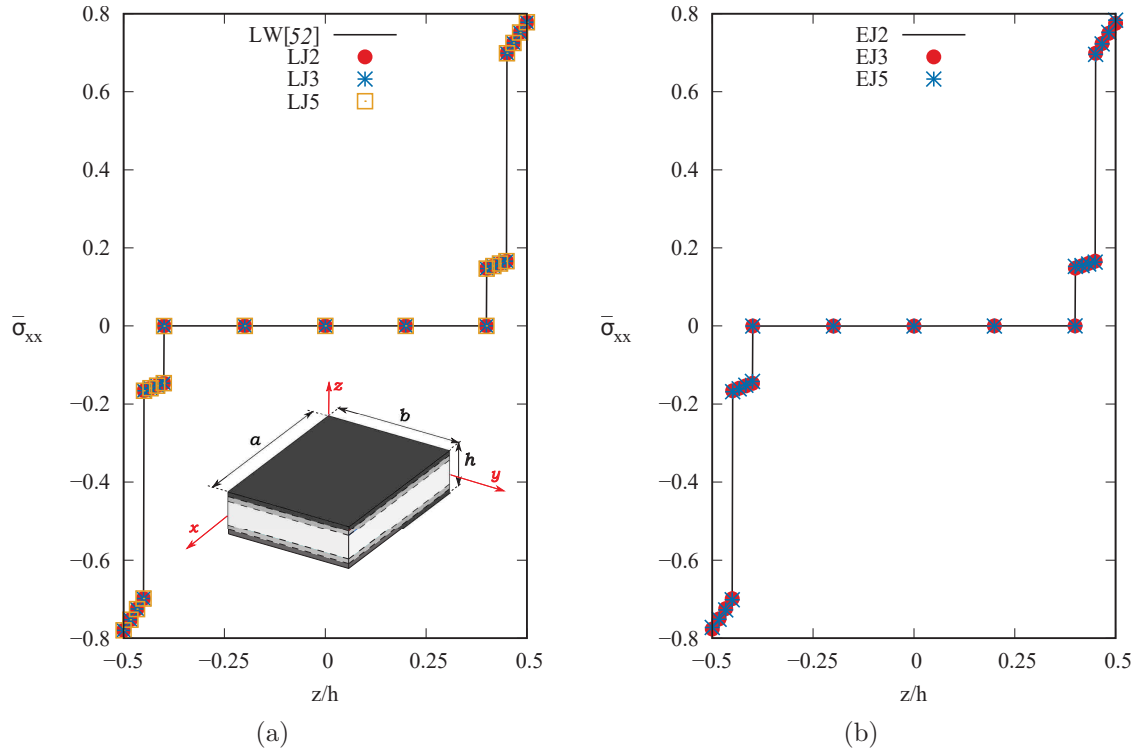
19

Figure 17: In-plane stresses in $[a/2, a/2, z]$ of five-layer composite sandwich with 2D formulation for LW (a) and ESL (b) models.
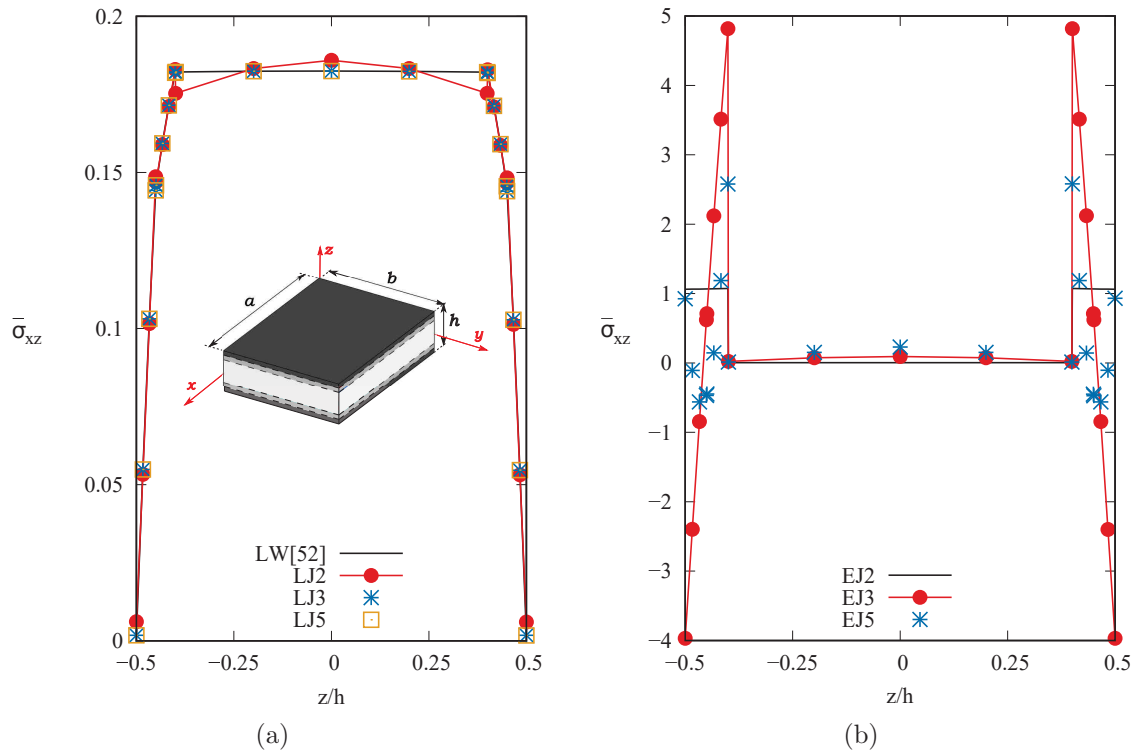

Figure 18: Shear stresses in $[a/2, a/2, 0]$ of five-layer composite sandwich with 2D formulation for LW (a) and ESL (b) models.

improve with the increasing of DOF. Excellent results are obtained for the LW models. The in-plane stresses are calculated well by LW models, while several problems can be found when adopting theories with fewer DOFs (see Table 9 and 19). As usual, the shear stresses are calculated with more difficulties. If results with the Hooke's Law are considered, classical and ESL theories are not able to be near to the reference solution. Better results are obtained with more refined theories (see Table 9 and Fig. 20). If the stress recovery method is used, less refined theories are improved greatly, whereas LW models almost fit perfectly with the reference solution(see Table Fig. 20). Secondly, a thinner shell $R_\beta/h = 10$ is analysed. Transverse displacements (see Table 9) are well obtained, except for CLT, FSDT, EJ1 and EJ2. Same considerations can be given for the in-plane stresses as shown in Table 9 and Fig. 21. Considering the shear stresses, there is an analogous behaviour to thick shell, even though ESL models are very near to the reference solution (see Table 9 and Fig. 22).

| Model | $R_\beta/h = 4$ | | | $R_\beta/h = 10$ | | | DOF |
	$\overline{u}_z$	$\overline{\sigma}_{\beta\beta}$	$\overline{\sigma}_{\beta z}$	$\overline{u}_z$	$\overline{\sigma}_{\beta\beta}$	$\overline{\sigma}_{\beta z}$	
Exact[54]	0.457	1.367	0.476	0.144	0.897	0.525	—
CLT[54]	0.0781	0.732	—	0.0777	0.759	—	—
Present Analysis(Layer-Wise)							
LJ1	0.440	1.199	0.478	0.141	0.853	0.525	2100
LJ2	0.454	1.334	0.471	0.144	0.883	0.523	3675
LJ3	0.458	1.354	0.475	0.144	0.884	0.524	5250
LJ4	0.458	1.354	0.475	0.144	0.884	0.524	6825
LJ5	0.458	1.354	0.475	0.144	0.884	0.524	8400
Present Analysis(Equivalent Single Layer)							
CLT	0.074	0.654	—	0.076	0.709	—	525
FSDT	0.293	1.318	0.178	0.112	0.721	0.184	875
EJ1	0.331	0.759	0.208	0.119	0.766	0.196	1050
EJ2	0.329	0.789	0.208	0.119	0.766	0.196	1575
EJ3	0.425	1.318	0.375	0.136	0.869	0.382	2100
EJ4	0.426	1.306	0.375	0.136	0.868	0.382	2625
EJ5	0.435	1.315	0.429	0.140	0.875	0.476	3150

Table 9: Transverse displacement,in-plane and shear stresses of three-layer composite shell under with 2D shell formulation. $\overline{u}_z$ calculated in $[a/2, b/2, 0]$, $\overline{\sigma}_{\beta\beta}$ calculated in $[a/2, b/2, h/2]$ and $\overline{\sigma}_{\beta z}$ calculated in $[a/2, 0, 0]$.

5   Conclusions

The present work evaluated the performances and benefits of adopting Equivalent Single Layer (ESL) and Layer-Wise (LW) approaches based on the Hierarchical Jacobi Expansion (HJ) in the static analysis of beams, plates and shells. Various geometries were analysed and one-dimensional (1D) beams, two-dimensional (2D) plates and shells were employed. Different kinds of pressures and geometrical boundary conditions were considered.

Four case studies were taken from well-known literature problems. Results are compared with reference solutions and classical models. The following main conclusions can be summarized as follows:
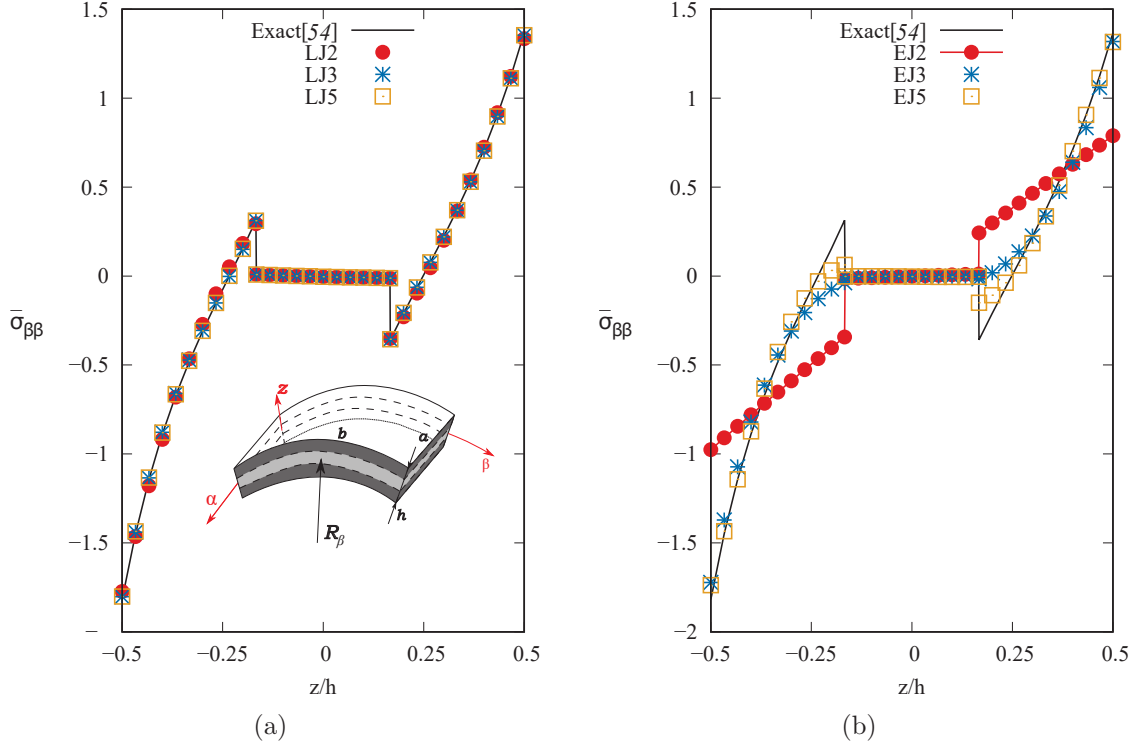
Figure 19: In-plane stresses in $[a/2, b/2, z]$ of three-layer composite shell with 2D shell formulation, for LW (a) and ESL (b) models, in case of $R_\beta/h = 4$.
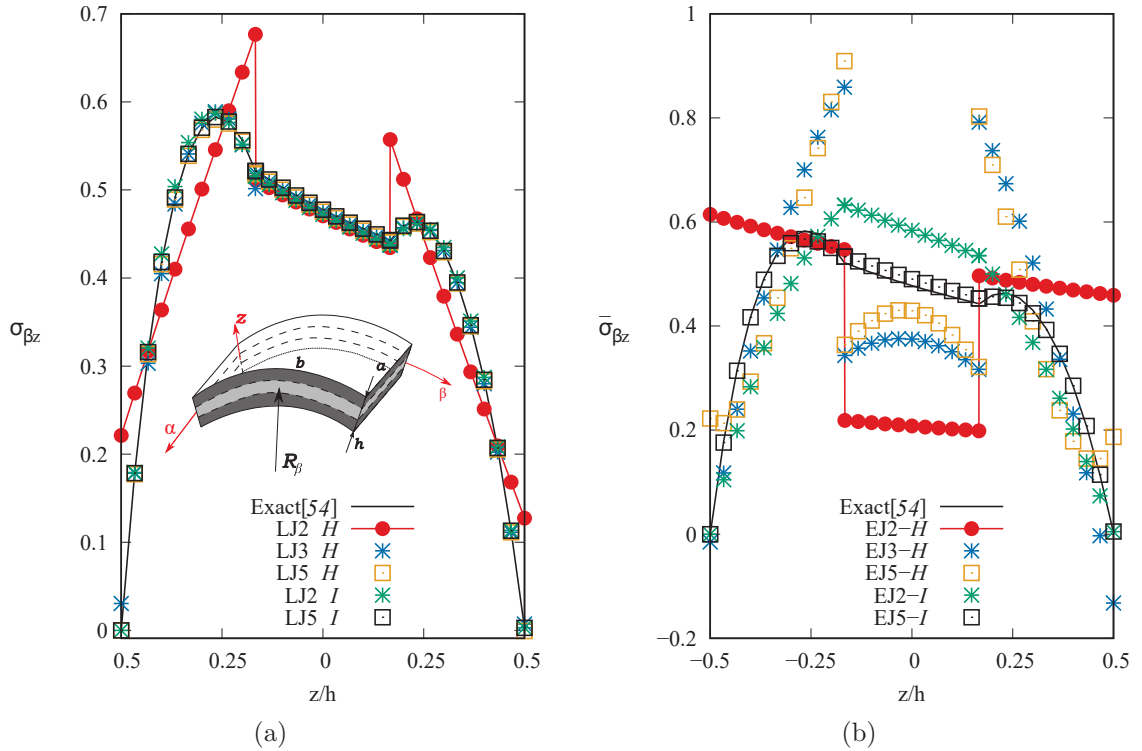

Figure 20: Shear stresses in $[a/2, 0, z]$ of three-layer composite shell with 2D shell formulation, for LW (a) and ESL (b) models, in case of $R_\beta/h = 4$.
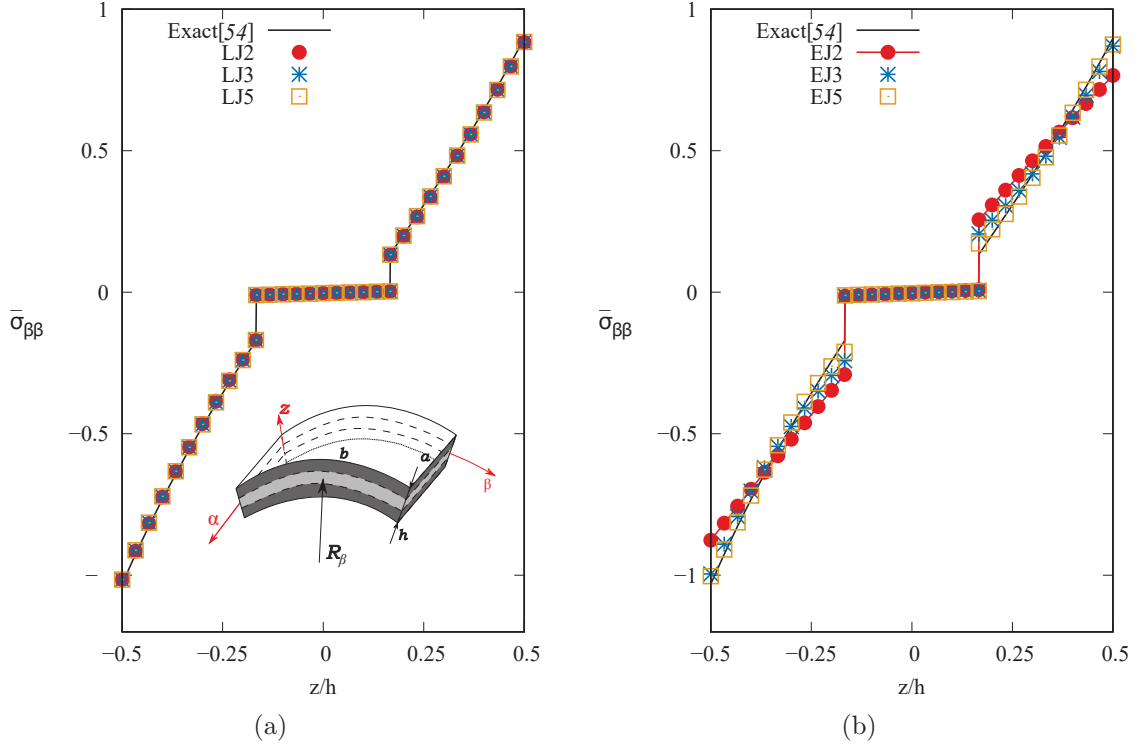
Figure 21: In-plane stresses in $[a/2, b/2, z]$ of three-layer composite shell with 2D shell formulation for LW (a) and ESL (b) models, in case of $R_\beta/h = 10$.
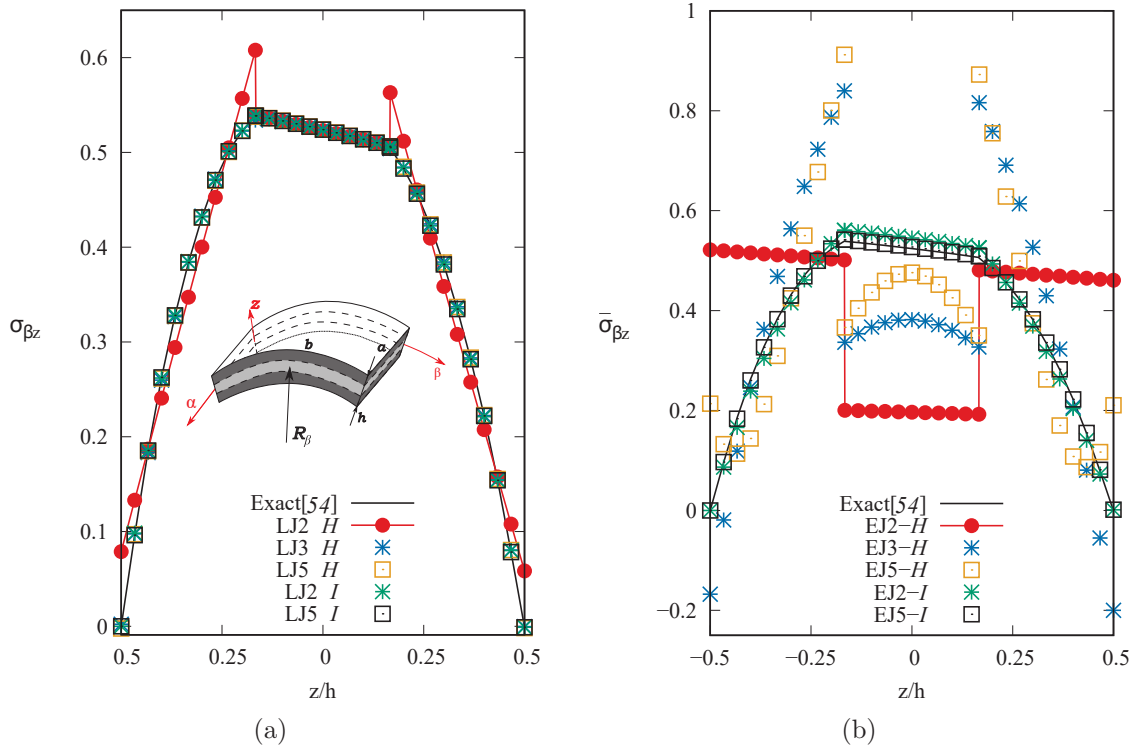

Figure 22: Shear stresses in $[a/2, 0, z]$ of three-layer composite shell with 2D shell formulation, for LW (a) and ESL (b) models, $R_\beta/h = 10$.

- Given a certain polynomial order, the parameters γ and θ of the Jacobi polynomials are not influential for the calculations.

- On the topic of shear locking, LW and ESL models with Jacobi polynomials produce similar trends when a convergence for displacements is performed.

- The proposed LW approach with Jacobi polynomials guarantees to obtain results close to the solutions from the literature. Given that LW approach has a high computational cost, it is sometimes useful to adopt the ESL approach. Furthermore, it gives better results than classical theories.

- The stress recovery method is able to resolve some of the critical issues presented in the calculation of the shear stresses, even for the low-order models.

Future works could be usefully devoted to free-vibration analysis and to the study of geometrical nonlinear applications.

References

[1] E. Carrera. Historical review of zig-zag theories for multilayered plates and shells. *Appl. Mech. Rev.*, 56(3):287–308, 2003.

[2] L. Euler. *Methodus inveniendi lineas curvas maximi minimive proprietate gaudentes sive solutio problematis isoperimetrici latissimo sensu accepti*, volume 1. Springer Science & Business Media, Berlin, Germany, 1952.

[3] S.P. Timoshenko. On the transverse vibrations of bars of uniform cross section. *Philosophical Magazine*, 43:125–131, 1922.

[4] V.V. Novozhilov. *Theory of elasticity*. Pergamon, Elmsford, 1961.

[5] R.K. Kapania and S. Raciti. Recent advances in analysis of laminated beams and plates. Part I: Shear effects and buckling. *AIAA journal*, 27(7):923–935, 1989.

[6] R.K. Kapania and S. Raciti. Recent advances in analysis of laminated beams and plates. Part II: Vibrations and wave propagation. *AIAA journal*, 27(7):935–946, 1989.

[7] Erasmo CARRERA, Alfonso PAGANI, Marco PETROLO, and Enrico ZAPPINO. Recent developments on refined theories for beams with applications. *Mechanical Engineering Reviews*, 2(2):14–00298–14–00298, 2015.

[8] V. Z. Vlasov. *Thin-walled elastic beams*. National Technical Information Service, 1984.

[9] R. D. Ambrosini, J. D. Riera, and R. F. Danesi. A modified vlasov theory for dynamic analysis of thin-walled and variable open section beams. *Engineering Structures*, 22(8):890–900, 2000.

[10] I. Mechab, N. El Meiche, and F. Bernard. Analytical study for the development of a new warping function for high order beam theory. *Composites Part B: Engineering*, 119:18–31, 2017.

[11] P.O. Friberg. Beam element matrices derived from vlasov's theory of open thin-walled elastic beams. *International Journal for Numerical Methods in Engineering*, 21(7):1205–1228, 1985.

[12] R. Schardt. Eine erweiterung der technischen biegetheorie zur berechnung prismatischer faltwerke. *Der Stahlbau*, 35:161–171, 1966.

[13] G. Kirchhoff. Über das gleichgewicht und die bewegung einer elastischen scheibe. *Journal für die reine und angewandte Mathematik (Crelles Journal)*, 1850(40):51–88, 1850.

[14] A.E.H. Love. *A treatise on the mathematical theory of elasticity.* Cambridge University Press, 1927.

[15] E. Reissner. The effect of transverse shear deformation on the bending of elastic plates. *Journal of Applied Mechanics*, 12:69–77, 1945.

[16] R. Mindlin. Influence of rotary inertia and shear flexural motion of isotropic, elastic plates. *Journal of Applied Mechanics*, 18:31–38, 1951.

[17] E. Reissner and Y. Stavsky. Bending and stretching of certain types of heterogeneous aeolotropic elastic plates. *Journal of Applied Mechanics*, 28:402–408, 1961.

[18] J.N. Reddy and D.H. Robbins Jr. Theories and computational models for composite laminates. 1994.

[19] E. Carrera. Developments, ideas, and evaluations based upon reissner's mixed variational theorem in the modeling of multilayered plates and shells. *Appl. Mech. Rev.*, 54(4):301–329, 2001.

[20] E. Carrera. Evaluation of layerwise mixed theories for laminated plates analysis. *AIAA journal*, 36(5):830–839, 1998.

[21] J.N. Reddy. A simple higher-order theory for laminated composite plates. *Journal of Applied Mechanics*, 51:745–752, 1984.

[22] H. Murakami. Laminated composite plate theory with improved in-plane responses. *Journal of Applied Mechanics*, 53(3):661–666, 09 1986.

[23] E. Carrera. Developments, ideas, and evaluations based upon reissner's mixed variational theorem in the modeling of multilayered plates and shells. *Applied Mechanics Reviews - APPL MECH REV*, 54, 07 2001.

[24] F.G. Rammerstorfer, K. Dorninger, and A. Starlinger. Composite and sandwich shells. In *Nonlinear analysis of shells by finite elements*, pages 131–194. Springer, 1992.

[25] J.N. Reddy. An evaluation of equivalent-single-layer and layerwise theories of composite laminates. *Composite structures*, 25(1-4):21–35, 1993.

[26] A.S. Mawenya and J.D. Davies. Finite element bending analysis of multilayer plates. *International Journal for Numerical Methods in Engineering*, 8(2):215–225, 1974.

[27] A.K. Noor and W.S. Burton. Assessment of computational models for multilayered composite shells. *Applied Mechanics Reviews*, 43.

[28] E. Carrera. Theories and finite elements for multilayered plates and shells: a unified compact formulation with numerical assessment and benchmarking. *Archives of Computational Methods in Engineering*, 10(3):215–296, 2003.

[29] E. Carrera, M. Filippi, and E. Zappino. Laminated beam analysis by polynomial, trigonometric, exponential and zig-zag theories. *European Journal of Mechanics - A/Solids*, 41:58–69, 2013.

[30] E. Carrera, M. Filippi, and E. Zappino. Free vibration analysis of laminated beam by polynomial, trigonometric, exponential and zig-zag theories. *Journal of Composite Materials*, 48(19):2299–2316, 2014.

[31] A. Pagani, E. Carrera, R. Augello, and D. Scano. Use of lagrange polynomials to build refined theories for laminated beams, plates and shells. *Composite Structures*, 276, 2021.

[32] M. Abramowitz and I. A. Stegun. *Handbook of Mathematical Functions with Formulas, Graphs, and Mathematical Tables.* Dover Pubblications, 1964.

[33] M. Marčoková and V. Guldan. Jacobi polynomials and some related functions. In *Mathematical Methods in Engineering*, 2014.

[34] B. Guo and L. Shen, J.and Wang. Generalized jacobi polynomials/functions and their applications. *Applied Numerical Mathematics*, 59(5):1011–1028, 2009.

[35] W. M. Abd-Elhameed. New formulae for the high-order derivatives of some jacobi polynomials: an application to some high-order boundary value problems. *ScientificWorldJournal.*, 2014.

[36] S. Beuchler and J. Schoeberl. New shape functions for triangular p-fem using integrated jacobi polynomials. *Numer. Math.*, 103:339–366, 2006.

[37] B. Szabo, A. Duester, and E. Rank. *The p-Version of the Finite Element Method*, chapter 5. John Wiley & Sons, Ltd.

[38] S. Beuchler and V. Pillwein. Sparse shape functions for tetrahedral ¡i¿p¡/i¿-fem using integrated jacobi polynomials. *Computing*, 80(4):345–375, sep 2007.

[39] F. Fuentes, B. Keith, L. Demkowicz, and S. Nagaraj. Orientation embedded high order shape functions for the exact sequence elements of all shapes. *Computers & Mathematics with Applications*, 70(4):353–458, 2015.

[40] E. Zappino, G. Li, A. Pagani, E. Carrera, and A.G. de Miguel. Use of higher-order legendre polynomials for multilayered plate elements with node-dependent kinematics. *Composite Structures*, 202:222–232, 2018. Special issue dedicated to Ian Marshall.

[41] B. Alanbay, R. K. Kapania, and R. C. Batra. Up to lowest 100 frequencies of rectangular plates using jacobi polynomials and tsndt. *Journal of Sound and Vibration*, 480:115352, 2020.

[42] A. Pagani, A.G. de Miguel, M. Petrolo, and E. Carrera. Analysis of laminated beams via unified formulation and legendre polynomial expansions. *Composite Structures*, 156:78–92, 2016. 70th Anniversary of Professor J. N. Reddy.

[43] E. Carrera, M. Cinefra, and G. Li. Refined finite element solutions for anisotropic laminated plates. *Composite Structures*, 183:63–76, 2018. In honor of Prof. Y. Narita.

[44] E. Carrera and S. Valvano. Analysis of laminated composite structures with embedded piezoelectric sheets by variable kinematic shell elements. *Journal of Intelligent Material Systems and Structures*, 28(20):2959–2987, 2017.

[45] E. Carrera, A. Pagani, and S. Valvano. Shell elements with through-the-thickness variable kinematics for the analysis of laminated composite and sandwich structures. *Composites Part B: Engineering*, 111:294–314, 2017.

[46] E. Zappino E. Carrera, M. Cinefra and M. Petrolo. *Finite Element Analysis of Structures Through Unified Formulation.* Prentice hall, John Wiley & Sons Ltd, 2014.

[47] K. J. Bathe. *Finite Element Procedure.* Prentice hall, Upper Saddle River, New Jersey, USA, 1996.

[48] T.J.R. Hughes. *The Finite Element Method: Linear Static and Dynamic Finite Element Analysis.* Courier Corporation, 2012.

[49] E. Carrera, G. Giunta, and M. Petrolo. *Beam structures: classical and advanced theories.* John Wiley & Sons, 2011.

[50] E. Carrera, R. Augello, and D. Scano. Use of esl lagrange theories for beams, plates and shells. *Atti dell'Accademia delle Scienze*, 2022.

[51] N.J. Pagano. Exact solutions for composite laminates in cylindrical bending. *Journal of Composite Materials*, 3(3):398–411, 1969.

[52] A. Pagani, S. Valvano, and E. Carrera. Analysis of laminated composites and sandwich structures by variable-kinematic mitc9 plate elements. *Journal of Sandwich Structures & Materials*, 20(1):4–41, 2018.

[53] M. Petrolo and A. Lamberti. Axiomatic/asymptotic analysis of refined layer-wise theories for composite and sandwich plates. *Mechanics of Advanced Materials and Structures*, 23(1):28–42, 2016.

[54] J.G. Ren. Exact solutions for laminated cylindrical shells in cylindrical bending. *Composites Science and Technology*, 29(3):169–187, 1987.

[55] O. C. Zienkiewicz, R. L. Taylor, and J. M. Too. Reduced integration technique in general analysis of plates and shells. *International Journal for Numerical Methods in Engineering*, 3(2):275–290, 1971.

[56] K.T. Kavanagh and S.W. Key. A note on selective and reduced integration techniques in the finite element method. *International Journal for Numerical Methods in Engineering*, 4(1):148–151, 1972.

[57] M. L. Bucalem and K.J. Bathe. Higher-order mitc general shell elements. *International Journal for Numerical Methods in Engineering*, 36(21):3729–3754, 1993.

[58] E. Carrera, A. G. de Miguel, and A. Pagani. Extension of mitc to higher-order beam models and shear locking analysis for compact, thin-walled, and composite structures. *International Journal for Numerical Methods in Engineering*, 112(13):1889–1908, 2017.

[59] E. Carrera. Single vs multilayer plate modelings on the basis of reissner's mixed theorem. *Aiaa Journal - AIAA J*, 38:342–352, 02 2000.